processes

MDPI

Review

Processing Methods Used in the Fabrication of Macrostructures Containing 1D Carbon Nanomaterials for Catalysis

João Restivo *, Olívia Salomé Gonçalves Pinto Soares and Manuel Fernando Ribeiro Pereira

Laboratory of Separation and Reaction Engineering—Laboratory of Catalysis and Materials (LSRE-LCM), Faculty of Engineering, University of Porto, 4200-465 Porto, Portugal; salome.soares@fe.up.pt (O.S.G.P.S.); fpereira@fe.up.pt (M.F.R.P.)

* Correspondence: jrestivo@fe.up.pt

Received: 1 September 2020; Accepted: 15 October 2020; Published: 22 October 2020

Abstract: A large number of methodologies for fabrication of 1D carbon nanomaterials have been developed in the past few years and are extensively described in the literature. However, for many applications, and in particular in catalysis, a translation of the materials to a macro-structured form is often required towards their use in practical operation conditions. This review intends to describe the available methods currently used for fabrication of such macro-structures, either already applied or with potential for application in the fabrication of macro-structured catalysts containing 1D carbon nanomaterials. A review of the processing methods used in the fabrication of macrostructures containing 1D sp2 hybridized carbon nanomaterials is presented. The carbon nanomaterials here discussed include single- and multi-walled carbon nanotubes, and several types of carbon nanofibers (fishbone, platelet, stacked cup, etc.). As the processing methods used in the fabrication of the macrostructures are generally very similar for any of the carbon nanotubes or nanofibers due to their similar chemical nature (constituted by stacked ordered graphene planes), the review aggregates all under the carbon nanofiber (CNF) moniker. The review is divided into methods where the CNFs are synthesized already in the form of a macrostructure (in situ methods) or where the CNFs are previously synthesized and then further processed into the desired macrostructures (ex situ methods). We highlight in particular the advantages of each approach, including a (non-exhaustive) description of methods commonly described for in situ and ex situ preparation of the catalytic macro-structures. The review proposes methods useful in the preparation of catalytic structures, and thus a number of techniques are left out which are used in the fabrication of CNF-containing structures with no exposure of the carbon materials to reactants due to, for example, complete coverage of the CNF. During the description of the methodologies, several different macrostructures are described. A brief overview of the potential applications of such structures in catalysis is also offered herein, together with a short description of the catalytic potential of CNFs in general.

Keywords: carbon nanofibers; nanostructured carbon; 1D carbon nanomaterials; catalysis; nanocatalysts; structured catalysts; catalyst preparation

1. Introduction

After the discovery of reproducible methods for fabrication of carbon nanomaterials in their various forms, the materials science and engineering community rapidly took up to their application in several fields. Their unique electronic and mechanical properties were shown early on to be extremely interesting for areas ranging from electronic and structural engineering to catalysis. Carbon nanomaterials have been synthesized and developed in several different allotropes, with 1D,

2D, and 3D geometries [1]; these morphologies are directly connected to the crystalline structure of the carbon lattices. 1D geometries have been the focus of particular interest due to the combination of electronic, textural, and mechanical properties. The sp2 hybridized carbon allotropes are characterized by the availability of π-electrons on the graphitic planes, contributing to their remarkable electronic and catalytic properties. 1D allotropes are particularly interesting in catalysis, and their preparation and application will be discussed in detail. 2D allotropes include, for example, graphene, and 3D allotropes include, for example, diamonds.

Carbon nanofibers can be defined as 1D carbon allotropes, which include carbon nanofibers and nanotubes. Their general morphology is characterized by a large aspect ratio between the diameter and the length of the fibers. The nano-classification is attributed to the nanoscale diameter of the fibers and the clearly defined structure at the nanoscale, with easily identifiable independent graphene planes.

Nevertheless, within this class, important differences are found between the most typical morphologies (Figure 1). Carbon nanotubes are conceptualized as (one or multiple) rolled-up graphene sheet(s), forming an empty shell cylindrical structure, and are usually classified regarding the number of graphene layers on their walls, either as single- or multi-walled carbon nanotube (occasionally double-walled is also used). However, it is important to note that the synthesis of the nanotubes is generally not carried out as a rolled-up graphene sheet, but rather grown by chemical vapor deposition of a carbon source over appropriate metallic nanoparticles. Carbon nanofibers are characterized by the absence of the tubular nanostructure of the nanotubes, consisting typically of a fishbone or platelet type arrangement, where graphene planes are stacked forming the 1D fibrous morphology (Figure 2). Certain synthesis methodologies can also produce carbon nanofibers with an amorphous crystalline structure, marked by the absence of graphitic sp2 carbon (Figure 2f).

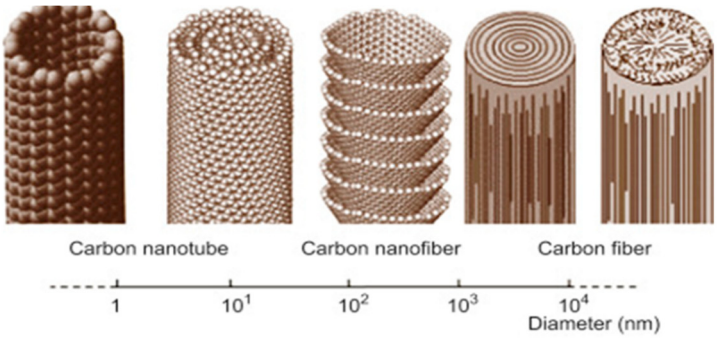

Figure 1. Morphology of 1D sp2 hybridized graphitic carbon allotropes and the relationship between fiber morphology and diameter inherent to the synthesis procedures [2].

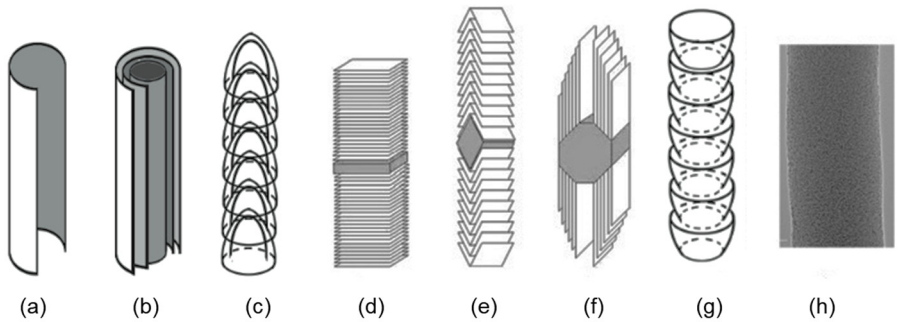

Figure 2. Details of the nanostructure of different types of carbon nanofibers: (**a**) single-walled nanotube; (**b**) multi-walled nanotube; (**c**) bamboo-like nanotube; (**d**) platelet; (**e**) fishbone; (**f**) ribbon; (**g**) stacked cup; (**h**) amorphous [3,4].

The 1D carbon nanofibers in their various morphologies share several properties that are relevant for their applications as catalysts, namely those linked with the presence of the sp2 hybridized graphitic

carbon planes in their structure. These are characterized by the presence of a high-density of delocalized π-electrons orbitals (Figure 3, highlighting the effect of bending of planar graphene taking place in 1D carbon nanomaterials and its effect on π-orbitals), which are responsible for the catalytic properties of graphene and other allotropes of the same electronic configuration [5,6].

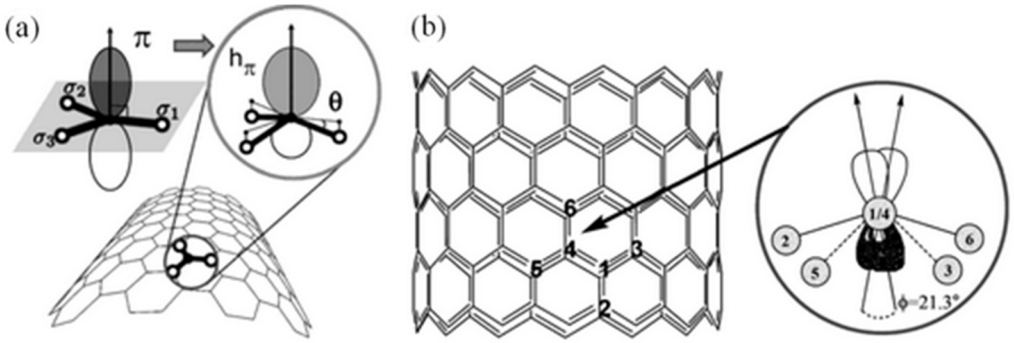

Figure 3. π-orbitals in planar graphene and changes under bending: (**a**) transformation into hπ and pyramidalization, and (**b**) misalignment angles [6].

On the other hand, these materials, including carbon nanofibers, can be finely tuned to the desired chemical and textural properties using methodologies already well-understood in application to traditional carbon materials (such as activated carbon). Such techniques included the modification of the surface chemistry through the introduction of heteroatoms (containing oxygen, nitrogen, sulfur, or phosphorous) on the surface of the carbons [7], or the modification of the textural properties using oxidative and thermal treatments [8]. It has been demonstrated that the same methods are effective and consistent in the modification of 1D carbon nanomaterials [9–14].

1D carbon nanomaterials also tend to form structures that, while presenting relatively large specific surface areas (up to 500 m^2/g), have a higher percentage of mesopores when compared with other traditional carbon materials, such as activated carbon, which is typically predominantly microporous [6,15]. The mesopores are formed by the entangled nanofibers creating intraparticle voids that are typically within this range (2–50 nm according to IUPAC [16]), depending on fiber morphology, packing, and alignment [17].

The common ground between the different 1D carbon nanomaterials is thus established by their shared characteristics, and most importantly, by their behavior during synthesis and application in macro-structured catalysts. Thus, for convenience, 1D carbon nanomaterials are here fit under the same umbrella using the name carbon nanofibers (CNFs).

The technological maturation of carbon nanofibers as catalysts relies on the development of solutions that allow their use in practical applications. The nanosized powders cannot generally simply replace other powders in large-scale reactors as difficulties regarding their handling will rise, such as increased pressure drops or further requirements for filtration of outlet flows. On the other hand, many concerns have been raised due to the harmful potential of carbon nanoparticles (and nanoparticles in general); carbon nanofibers are at the center of this debate due to their large aspect ratio and small dimensions [18–23]. Thus, it is clear that the use of carbon nanofibers as catalysts in practical applications will require the development of robust techniques for their immobilization. In here, we describe and discuss a series of methods available to prepare macro-structures containing immobilized carbon nanofibers and their application as catalysts. The following sections are divided into the methods where the CNFs are synthesized already in the form of a macrostructure (in situ methods) or where the CNFs are previously synthesized and then further processed into the desired macrostructures (ex situ methods). We highlight in particular the advantages of each approach, including a (non-exhaustive) description of the methods commonly described for in situ and ex situ preparation of the catalytic macro-structures.

2. Application of Carbon Nanofibers Immobilized on Macro-Structures in Catalysis

2.1. Carbon Nanofibers in Catalysis

The techniques previously described for modification of the surface chemistry of carbon materials have been used to improve the catalytic performance of CNFs in a large number of different reactions. The introduction of oxygen-containing functionalities has been demonstrated in carbon nanofibers, and their effect on their activity as catalyst or as catalyst support has been tested in several reactions, including ozonation [24] and catalytic wet air oxidation [25] of water contaminants, in fuel cell electrodes [26,27], nitrate [28], nitrobenzene [29,30], naphthalene [31], cinnamaldehyde [32,33], phenylacetylene [34] hydrogenation, nitrous oxide reduction [35], electrocatalytic oxygen reduction [35], methanol oxidation [36], Fischer–Tropsch reaction [27], and others [5]. Similar studies have been carried out when using other elements as dopants, such as nitrogen [37–47], boron [38,45,48], potassium [27,38,49], fluorine [50,51], phosphorous [45], or sulfur [52–54]. Nevertheless, the various morphologies of the 1D carbon nanofibers illustrated in Figure 2 may offer particular characteristics of interest to specific catalytic applications, in particular the potential presence of a large number of defects on the carbon lattice of the carbon nanofibers when compared with carbon nanotubes (Figure 2a) is of interest for certain reactions [55]. Catalytic and electrocatalytic reactions can benefit from the presence of defects as active reaction or adsorption sites [56], or as sites for doping with reactive metallic nanoparticles [57].

In fact, following on from the traditional application of activated carbon in catalysis, carbon nanofibers may be used as supports for active metallic catalytic phases. The electronic and textural properties of the 1D carbon nanofibers have been shown to be useful in improving the catalytic activity of metallic catalysts when compared with other traditional supports, due to their high external surface area [58] and low interaction between the impregnated metallic phase and the exposed planes of the support, which leads to the formation of active metallic faces [59]. Supported metallic catalysts have been shown to have improved efficiency in various applications, including as electrocatalysts in PEM fuel cells [59] and methanol fuel cells [60], in Fischer–Tropsch reactions [61], catalytic wet air oxidation of contaminated wastewater [62], methane decomposition [63], and in hydrogenation of organic compounds [64].

Finally, the particular textural properties of CNFs are beneficial in some catalytic applications where the accessibility and availability of the active catalytic sites can be enhanced in comparison with the case of microporous materials [65,66].

2.2. Macro-Structures in Catalysis

The development of structured catalysts originated long before the introduction of carbon nanofibers, or nanomaterials in general, to catalysis. The automotive catalyst is the most common example of the wide-scale use and mass production of a structured catalyst. These catalysts consist of honeycomb supports (cordierite, silicon carbide, or metallic alloys) coated with the required catalytic layers. The honeycomb structure was designed and adopted as the industry standard due to the beneficial compromise between surface contact area and low-pressure drop. In fact, low-pressure drop is a crucial requirement for the automotive industry, as it directly relates to the fuel efficiency of the internal combustion engines [67]. Additionally, the monolith honeycomb structure offers improved handling of heat exchange, and, thus, has been adopted by the industry for other types of catalytic reactions, including CO oxidation [68], gas steam reforming [69], Fischer–Tropsch synthesis [70], among many others. It is also worth noting the application of the honeycomb monolith catalyst in multi-phasic applications. These consist of the combination of the solid phase catalyst and reactants in different phases (gas and liquid) simultaneously flowing through the monolith channels. This setup offers an additional advantage to those listed above as it promotes the formation of specific hydrodynamic regimes that enhance mass transfer between the three phases (commonly referred to as Taylor flow, bubble train flow, or slug flow) [71].

Another common type of catalytic macro-structured support is foam. The foam structure with controlled porosity can be advantageous as it allows the design of catalytic systems with carefully designed relationships between pressure drop and contact area [72,73]. Moreover, foams can also offer excellent heat exchange capabilities, depending on material selection and pore structure [74].

Pellets are also often used in place of powders in packed bed reactors. Pellets are formed as compressed catalytic material, resulting in several individual particles ranging in size from several hundred micrometers to a few centimeters. The shape of the pellets can also be adjusted according to requirements. The advantages of pelletization include the formation of a porous catalytic packed bed with the possibility of adjusting the compromise between the pressure drop and surface contact area, and less strict requirements for filtration for separating or recovering the catalytic material [75,76]. The same principle can be applied to other inert supports with similar shapes and sizes to the catalyst pellets, when coated with catalytic material [77].

Membranes have also been applied as catalyst support, most commonly in gas phase reactions or electrocatalysis. Recently, the combination of filtration with catalytically active membrane materials has led to the development of catalytic membranes for water treatment and other liquid phase reactions [78]. The membrane configuration can be used to promote the contact between the gas/liquid phases and the catalytic solid phase, or to promote separation between the reactants and or products during the reaction [79–81].

CNF films, on the other hand, have seen several different applications in electrochemistry, mostly for electrode coating [82,83] and in sensors [84].

A description of techniques used in the preparation of catalytic structures using carbon nanofibers is presented in the following sections. The methods are separated by whether the CNFs are produced I situ by carbonization of polymeric precursors or decomposition of gaseous carbon sources over metallic catalysts, or ex situ, where the CNFs are fabricated using conventional methodologies in powder form and processed post-synthesis to obtain CNF structures following a number of different approaches.

The methods include those used in the fabrication of flat structures (membranes and films) and bulky structures (foams and coated supports). Where appropriate, methods reported in the literature for non-catalytic applications but with relevance to the topic at hand are cited. Additionally, it is worth noting that a large number of reports exist on the use of carbon nanofibers as fillings for structural engineering, which are not discussed in this work due to their incompatibility with catalysis (generally due to low amounts of the nanofillers, or their complete coverage by other materials).

3. In Situ Preparation of CNF Structures

3.1. Electrospinning

The synthesis of fibers and nanofibers by electrospinning is an adaptation of the dry spinning technique used for the production of polymer fibers [85]. The introduction of an electric potential between the polymer nozzle and the substrate allows control of the diameter of the viscoelastic jet through electrostatic repulsion between the surface charges, which in turns makes possible the synthesis of polymeric nanofibers. Such additional control of the fabrication conditions is reflected in the fine tuning of the nanofibers' characteristics, including morphology (both size and aspect ratio), composition, secondary structures, and spatial alignments [86]. The general methodology consists of the preparation of a polymer solution that is fed through a needle into a nozzle that delivers the solution onto a substrate. The nozzle and substrate are operating at an electric difference of potential (in the 10–20 kV range). The fibers are collected on the substrate and carbonized under an inert atmosphere. Depending on the polymer of choice, a stabilization step might be required before carbonization. Variations to the process are introduced towards achieving fibers with specific characteristics as required for the target application; Figure 4 details a general approach to electrospinning of a PAN (polyacrylonitrile)-based CNF using sacrificial SiO_2 nanoparticles to achieve surface mesoporosity, with SEM images of the resulting membrane at varying magnifications [87].

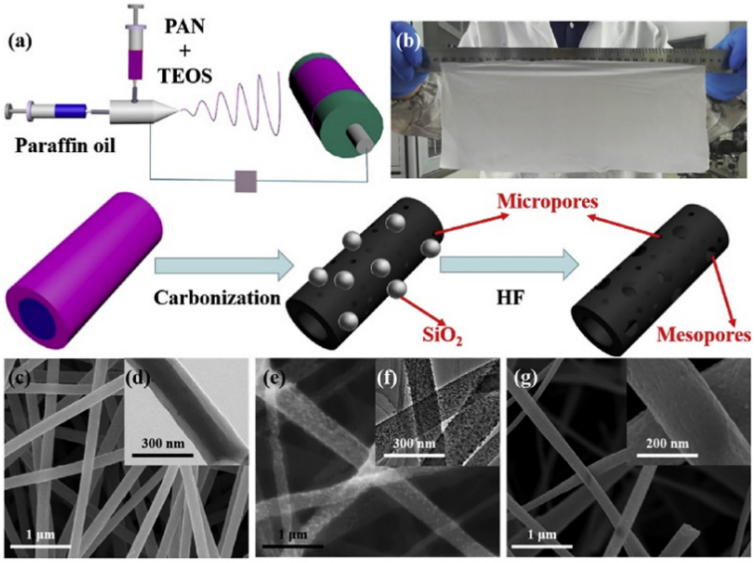

Figure 4. Example of carbon nanofiber (CNF) membrane fabrication using a polyacrylonitrile (PAN) precursor by electrospinning and carbonization, with sacrificial SiO_2 doping to achieve controlled mesoporosity; (**a**) schematic illustration of the synthesis of PCCNF. (**b**) digital photo of paraffin oil@PAN/TEOS. (**c**) SEM image and (**d**) TEM image of paraffin oil@PAN/TEOS. (**e**) SEM image and (**f**) TEM image of hollow carbon/SiO_2. (**g**) SEM image of PCCNF [87].

Electrospinning is often used to prepare CNF membranes. However, the technique has also been used to fabricate free-standing CNF films using a process very similar to that for fabrication of membranes [88–90]. The difference is found in the characteristics of the material (e.g., thickness, dimensions, or fiber density), but in most cases the nomenclature is closely related to the final application of the film or membrane. Nevertheless, electrospinning can also be used to prepare fibers in powder form [86], which can again be achieved by fine control of the synthesis conditions.

A number of polymeric precursors have been reported for the manufacture of membranes for posterior carbonization and activation. The precursors are selected based on their adaptability to form both the nanofiber membranes by electrospinning and graphitic carbon upon carbonization and activation. Polyacrylonitrile (PAN) is commonly used as the formation of PAN membranes by electrospinning is fairly well understood and reproducible. Moreover, PAN solutions are very well suited for spinning applications and have a high carbon yield [91]. Generally, a PAN solution is prepared using an adequate solvent (for example, *N*,*N*-dimethyl formaldehyde, DMF, or dimetyhlsulfoxide, DMSO) and stirred at a low temperature to obtain a homogeneous mixture. The solution is then sprayed onto an inert target substrate (e.g., aluminum foil) using a syringe through a capillary tip. A difference in electrical potential is created between the syringe and a metal collector who holds the target substrate where the electrospun fibers are collected, forming a membrane. These are then stabilized, carbonized, and eventually activated, to form carbon nanofibers. The properties of the carbon nanofiber membranes are related to the conditions used in the various preparation stages, as summarized in Table 1. Further modifications can be carried out to alter the property of the fibers, including changes to the carbon surface chemistry and texture [92].

Table 1. Summary of the reported preparation methods of carbon nanofiber membranes and free-standing films by electrospinning.

Precursor	Solvent	Concentration	Additive	Voltage (kV)	Stabilization (°C)	Carbonization/Activation (°C)	Morphology	Reference
PAN	DMF	14 wt.%	-	20	280	600 in N_2, 750 with water steam	0.25 (0.24 micropores)	[93]
PAN	DMF	10 wt.%	-	20	280	800 in N_2, 800 with water steam	0.23 (0.21)	[94,95]
PAN	DMF	1 g in 5 mL	Graphene oxide	20	250	950 for 2 h in N_2	-	[96]
PAN	DMF	1 g in 9 mL	-	20	-	500 for 2 h in N_2	-	[97]
PAN	DMF	4–12 wt.%	TEOS	25–30	280	800–1000	~0.8 um (beads)	[98]
PAN	DMF and paraffin oil	0.9 g each in 10 mL	TEOS	16	-	1000 in Ar	205 ± 8 nm diameter and 3–7 nm mesopores	[87]
PAN	DMF	500 mg in 5 mL	Graphene oxide nanoribbon/carbon nanotube	20	250	700 in a reducing atmosphere (H_2/Ar, 5%/95%, *v*/*v*)	200–300 nm diameter (SEM)	[99]
PAN	DMF	0.5 g in 5 mL	-	18	300	900 in N_2 and using PAN decomposition tail gas	204 ± 26 nm	[100]
PAN	DMF	3.5 g in 50 mL	Cellulose acetate	55	280 in air	800 in N_2	200 to 500 nm (diameter) with channel rich structures (SEM)	[101]
PAN	DMF	1.6 g in 10 mL	ZIF-8 cubic nanoparticles	10.4	250 in air	900 in N_2	Hollow carbon nanofibers with 500 nm diameter	[102]
PAA	DMA	12 wt.%	Aniline	18–25	100/200/300	1000	140–215 nm (diameter SEM)	[103]
PS	DMF	25 wt.%	Dopamine	12	60 in vacuum	700 in Ar	2–4 um diameter (SEM)	[104]
PAN and PVP	DMF	PAN: 10 wt.% and PVP: 8 wt.%)	Terephthalic acid (PTA)	16	200–250	800 in N_2	1–2 um diameter (SEM)	[105]
SF	water	8 wt.%	-	20	350	800 in N_2	250 nm (diameter SEM)	[106]
PR	ethanol	22 wt.%	Fe (acetylacetonate)$_3$	-	-	Up to 900 under NH_3	Abundant micropores and narrow mesopore size distribution (3–10 nm)	[107]

Other polymers are available and reported in the literature, as listed in Table 1, such as polystyrene (PS), silk fibroin (SF), phenolic resin (PR), or poly(amide acid) (PAA). The use of alternative precursors aims at replacing the complex and sensitive stabilization steps required for PAN membranes while maintaining their excellent properties [106]. A hybrid approach has also been reported for the synthesis of carbon nanofiber containing membranes by electrospinning. For this, a similar procedure for the preparation of the membrane is followed, but the carbon nanofibers are added to the precursor solution prior to the membrane formation; the post-spinning carbonization step is not carried out. Thus, the method results in polymeric membranes containing carbon nanofibers, providing a hierarchically structured membrane [108].

The characterization of the CNF membranes' morphology is noticeably inconsistent with many reports employing exclusively one method, between textural characterization techniques (e.g., isothermal nitrogen adsorption), porosimetry characterization techniques (e.g., mercury porosimetry or known-size bead retention), and microscopy imaging. This is likely due to the differences in the target applications. Nevertheless, systematic reports have shown that the morphology and general characteristics of the membranes are affected by the preparation conditions.

3.2. Chemical Vapor Deposition

The preparation of CNF powders is generally carried out using a chemical vapor deposition method; this is particularly true for carbon nanotubes, which require finely controlled synthesis conditions [2]. The same methodology is also often applied to prepare both 2D and 3D CNT structures by using adequate supports for the growth catalysts [109]. A common example is the growth of CNF on a membrane support, as demonstrated for the catalytic hydrogenation of nitrite in water (Figure 5) [110], or the growth of CNF layers in cordierite honeycomb monoliths [111]. Nickel nanoparticles were deposited on the ceramic supports (membrane or honeycomb monolith) and the growth of CNF was carried out through thermal decomposition of a gaseous carbon source. The CNF are grown by decomposition of hydrocarbons (e.g., ethane, ethylene, methane) on the nickel (or other suitable metallic catalyst) particles under a reducing atmosphere.

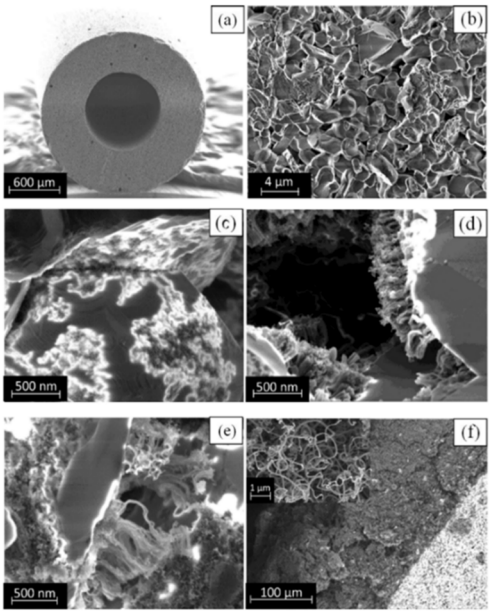

Figure 5. CNF film grown on a hollow alumina fiber; (**a**) low magnification and (**b**) high magnification SEM images of the hollow alumina fiber; CNF grown on alumina fiber using different Ni solutions: (**c**) 0.02 g/L, (**d**) 0.2 g/L, (**e**) 1.0 g/L, and (**f**) 5.0 g/L. [110].

A summary of the methodologies used in the preparation of CNF 2D and 3D structures by the growth of a CNF film is presented in Table 2, where the methods for the growth catalyst deposition and CNF growth are detailed.

Table 2. Summary of the preparation methods of carbon nanofiber films on macro-structured supports by chemical vapor deposition.

Growth Catalyst	Catalyst Film Deposition	Carbon Source	Thermal Decomposition (°C)	Additives	Morphology	Reference
Ni	Laser annealing of a thin nickel film obtained by electron beam sputtering	Ethylene	Ar ion laser operated at 488 nm	-	12–47 nm diameter, disordered film	[109]
Co	Electrodeposition on pores of porous anodic aluminum oxide	Acetylene	640	-	85 nm diameter in aligned CNF forest	[112]
Ni	Evaporation and sputtering on fused silica and silicon substrates	Ethane	700	-	50–10 nm diameter, disordered film	[17]
Ni	Micropattern formation by direct photolithography	Acetylene	600	-	20–40 nm diameter, aligned forests	[113]
Ni	500 nm diameter circular dots photolithographically defined on Si wafer	Acetylene	Plasma enhanced at 700	ammonia	conically shaped fibers of 6–20 μm length with tip diameters of 20–50 nm and base diameters of 500–600 nm	[114]
Ni	Ion beam coating of graphite paper with 22 nm thick Ni film	Acetylene	Plasma enhanced at 700	ammonia	Uniform vertical alignment at 50 to 250 nm diameter	[115]
Ni	100 nm diameter Ni spots using e-beam lithography	Acetylene	Plasma enhanced at 700	ammonia	Conically shaped fibers with height of 1.5 μm, a base diameter of 100 nm, and a tip diameter of 70 nm	[116]
Ni	Ni/Ta thin film (25 nm/10 nm) by electron-beam evaporation	Ethane	635	-	Highly entangled morphology of CNFs, diameters in the range 10–100 nm	[117]
Pt	2–10 nm film on n-type Si (100)/Ti (20 nm)/ta-C (7 nm) using cathodic arc deposition	Acetylene	Plasma-enhanced at 750	ammonia	Vertically aligned fibers that were ~0.2–1 μm tall	[118]
Ni	Thin films of Ni (5 nm) over Pd (200 nm) with a Ti adhesion layer deposited by e-beam evaporation	Ethane	Pre-heated gas at 770	-	Bidirectional growth of CNFs with embedded catalysts and diameters ranging from 70–160 nm with an average of 105 nm	[119]

Table 2. *Cont.*

Growth Catalyst	Catalyst Film Deposition	Carbon Source	Thermal Decomposition (°C)	Additives	Morphology	Reference
NiFe	NiFe sputter deposited on silicon substrates pre-coated with Cr, W, Ti, or Ta metal buffer layers	Methane	Hot filament at 1900–2050 and substrate temperature: 650–750	-	Un-aligned CNT	[120]
Ni	Electroplating	Methane	Hot filament at 1900–2050 and substrate temperature: 650–750	-	CNF films	[120]
Fe	Gaseous $Fe(CO)_5$	Acetylene	750	-	Aligned CNT	[121]
Fe	Gaseous $Fe(CO)_5$	Methane	1100	-	Un-aligned CNT	[121]
Fe	In situ decomposition of ferrocene	Toluene	550 and 940	-	Aligned CNT from 590 °C and above until 940 °C, 10–70 nm diameter	[122]
Ni-Fe	Sputtering of Fe_3Ni_2 over Si wafer	Acetylene	500	-	25 nm diameter	[123]
Ni-Cu	Sputtering of NiCu over Si wafer	Acetylene	400	-	58 nm diameter	[123]
Pd-Se	Se deposited by effusion cell, Pd deposited by electron beam evaporation	Acetylene	500	-	13 nm diameter, large number of defects	[123]

A typical top- and cross-sectional view of an entangled CNF layer is included in Figure 6, which is representative of the general morphology of the CNF films grown by chemical vapor deposition. The variations in the CVD method presented in Table 2 highlight how the CNF morphology is affected by the experimental conditions, ranging from catalyst selection and preparation to the temperature and method for thermal decomposition of the carbon source. Several authors have provided systematizations of the impact of several factors in CNF growth by CVD [124], e.g.,

- choice of carbon source: linear hydrocarbons (methane, ethylene, acetylene) form straight CNF, while cyclic hydrocarbons (benzene, toluene, xylene) form relatively curved CNF;
- catalyst particle size controls the fiber diameter;
- catalyst selection influences shape and size depending on their carbon diffusion rates (Fe, Ni, and Co have excellent such rates);
- substrate–catalyst interactions are determinant to maintain a stable and uniform catalyst particle size and thus uniform formation of CNF.

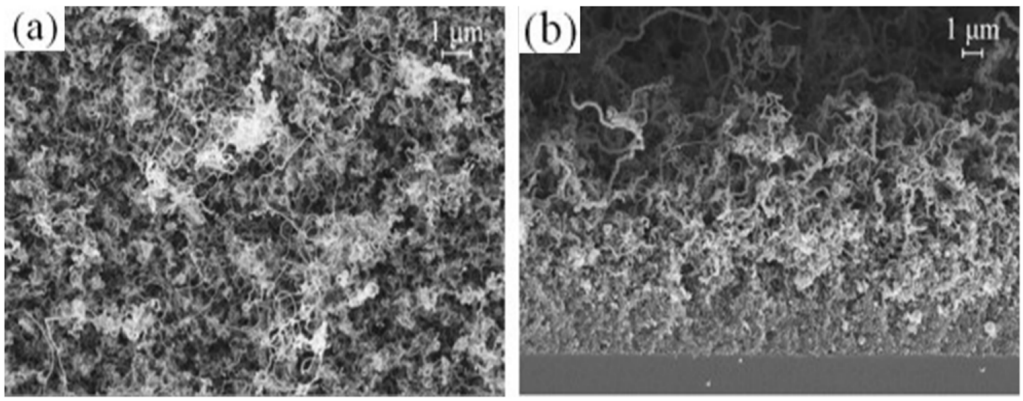

Figure 6. HR-SEM images illustrating the morphology of a highly-entangled CNF layer grown on 25 nm Ni and 10 nm Ta on oxidized silicon: (**a**) top-view; (**b**) cross-sectional view [117].

Chemical vapor deposition can also be used to form free-standing 3D structures containing CNF, namely foam-like structures. A foam-like lightweight structure was prepared using Fe in ferrocene as a catalyst for CNF growth and toluene as the carbon source. Boron is added in the form of benzeneboronic acid to promote the formation of stable bends in the CNF, resulting in mechanically flexible, ultra-light weight, free-standing foams [53]. A similar method was carried out for another boron-containing foam-like structure, where aerosol-assisted CVD was used to deliver the precursor mixture to the heated quartz tube reactor [125]. Aerosol-assisted CVD has also been used to form self-standing or substrate-supported CNF networks after transfer using a dry press technique. The formation of the networked films was achieved by collecting the CNF bundles on a membrane filter at the outlet of the CVD reactor [126]. A similar methodology for CNF network formation was used to form CNF containing fibers by a wet pulling technique using ethanol as a solvent; the resulting fibers can be subsequently woven into a macro-structure with potential for application as a catalyst [127].

4. Ex Situ Preparation of CNF Structures

The main challenges associated with the ex situ preparation of CNF structures are related to the requirement to obtain homogenous CNF dispersions on the solvents of choice, and to promote the formation of mechanically robust free-standing films capable of withstanding environments with harsh chemical and physical conditions. These have been achieved using both chemical and physical modification of pre-formed CNF. The following sections described how these are used to prepare suitable CNF dispersions, robust CNF structures, and how different ex situ preparation techniques are used to form 2D and 3D structures.

4.1. Preparation of Stable CNF Dispersions

Water-based CNF suspensions are generally unstable due to their hydrophobic nature inherent to their non-polar characteristics [128]. It is possible to introduce modifications to the chemistry of the CNF surface that induces a hydrophilic behavior. One approach is the surface functionalization with surfactants/dispersants that form a hydrophilic layer around the individual fibers or fiber agglomerations (Figure 7) [129]. Such compounds are generally characterized by their dual hydrophobic/hydrophilic character, which promotes the formation of hydrophilic layers that sustain the CNF dispersion in water. Among those reported in the literature, the most commonly used are Triton X-100™ and sodium dodecyl sulphate, but many other ionic (e.g., sodium 4-dodecylbenzenesulfonate, hexadecyl(trimethyl)azanium bromide) and non-ionic alternatives are available (Pluronic® F127 and F68) [130]. Functionalization with surfactants (sometimes described as physical functionalization [129]) has often been used in the preparation of CNF membranes and films by vacuum filtration [131–138]. For applications where the contact of reactants with the graphitic carbon surface is essential (e.g., catalysis), additional processing is required to remove the surfactant layers and any excess surfactant material, which can be achieved by washing with purified water [131], organic solvents [139], or thermal treatment [140].

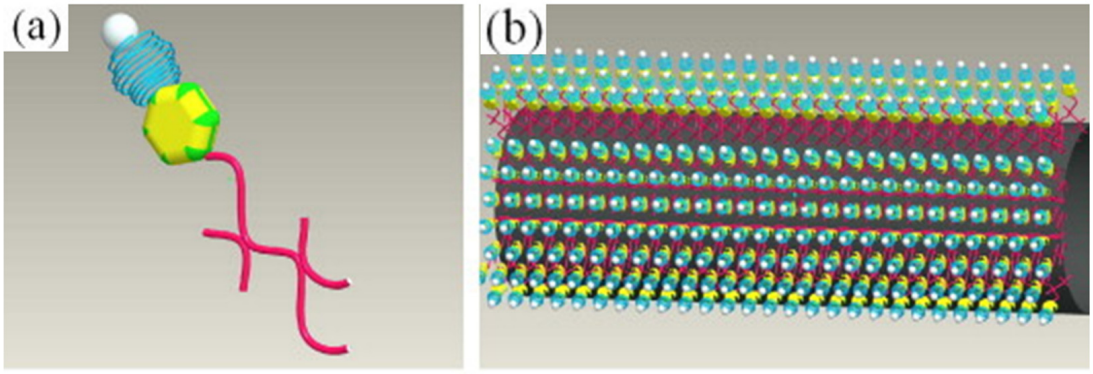

Figure 7. Functionalization of a CNF with the Triton X-100™ surfactant: (**a**) single molecule with hydrophilic head (top) and hydrophobic tail (bottom); and (**b**) formation of a uniform hydrophilic layer around the individual CNF [141].

The chemical functionalization of the CNF carbon surface with acidic oxygen-containing functionalities has also been shown to increase their hydrophilicity [142]. The oxidation of carbon with boiling nitric acid is the most common method for introduction of these surface groups [143]; other gas and liquid phase methods exist such as liquid phase ozonation [144] or thermal treatments under oxidizing atmospheres [145]. The hydrophilic nature of the oxidized CNF is attributed to the acidic nature of the groups introduced during oxidation, such as carboxyls, phenolic hydroxyls, and lactones. When the carbon material is suspended in a solution with pH higher than the pH at the point of zero charge (pH_{pzc}), the surface becomes negatively charged due to the deprotonation of the surface groups. The electrostatic repulsion between the particles then hinders the formation of large agglomerates that tend to precipitate out of suspension [31]. Conversely, doping with basic groups (e.g., amides) tends to lead to less stable dispersions. Similar to physical functionalization, it might be necessary to remove or further tune the surface chemistry of the CNF post-structuralization, depending on the target use. For catalytic reactions, whether using carbon as a catalyst or as catalyst support, it is well-understood that its surface chemistry plays a crucial role in defining its catalytic performance [146]. Thus, further treatments can be employed, e.g., thermal treatment under an inert atmosphere to remove surface oxygen-containing functional groups for reactions favored by a basic surface [140].

Polymer wrapping is another physical functionalization method used to stabilize CNF suspensions, in particular in the preparation of CNF–polymer composites. The linkage of a polymer to the CNF surface is promoted by introduction of carboxylic functional groups that allow the formation of

covalent bonds [147,148]. Other less common methods have been reported to stabilize CNF suspensions, including graphene blending [149] and DNA wrapping [150].

Mechanical or physical methods have also been used to promote de deagglomeration of CNF bundles in suspension. The use of ultrasonic processing (using baths or tips) has been shown extensively to promote the formation of more stable suspensions by untangling larger bundles prone to precipitation by gravity [139]. The modification of CNF morphology by milling has also been reported to improve the stability of suspensions, which has been attributed to the disentanglement of the CNF bundles [151] and a reduction in fiber lengths [152]. Separation of large bundles by centrifugation has also been used to obtain suspensions with only stably dispersed particles [153].

The combination of the above methods has also been shown to cumulatively improve the stability of the CNF suspensions. Mechanical methods are successful in untangling large CNF bundles and forming smaller particles by reducing the fiber lengths, while chemical methods hinder the re-agglomeration processes leading to precipitating of large CNF bundles [140,152].

Organic solvents can also be used to form stable CNF suspensions [154]. A study of the Hansen solubility parameters showed good dispersion and stability in solvents, with the values of the dispersive components within the range found for solvents with a moderate or low hydrogen-bonding strength [155]. *N*,*N*′-dimethylformamide (DMF) is a very common example of an organic solvent able to very efficiently disperse CNFs.

4.2. Improving the Robustness of Free-Standing CNF Structures

The preparation of free-standing CNF structures (and films to some extent) is severely limited by the mechanical resistance of the structure. On one hand, the use of CNF as filler in polymer and ceramic materials is well-known to improve the composites' mechanical properties [156,157]. However, in such formulations, the carbon materials are not able to act as catalysts due to their complete insertion into the composite matrix. Thus, methods to improve the mechanical properties of catalytically active structures are required.

Different approaches have been reported to promote the formation of covalent bonding between CNFs. These include the free-radical polymerization of allylamine functional groups using azobisiobutyronitrile as a radical initiator [158]. Another similar approach uses benzoyl peroxide as a radical initiator, achieving close control of the porosity of the nanostructure [159]. Suzuki coupling can also be used to form covalent bonding between the individual nanotubes using palladium chloride surface complexes that catalyze the formation of covalent bonds from boronic acid [160]. Boron and graphene have been reported as promoting the creation of nanojunctions between CNFs (Figure 8) [125]. Graphene has also been reported as efficient in forming junctions in pre-formed CNF macrostructures, namely aerogels [161]. A pre-formed macro-structure is coated with a polyacrylonitrile polymer that is then pyrolyzed to form graphene in situ. Agglomerations of graphene are found in the junctions between the nanotubes, improving the macro-structure mechanical properties. Hot-pressing of CNF films has also been used to improve the stability of the free-standing flat structures [162].

Adhesion of CNFs to support structures is also a concern regarding producing structured catalysts able to withstand harsh reaction conditions. The modification of the supporting structure or substrate and/or of the CNF can be used to enhance the robustness of such films. Hydrogen bonding has been proposed as an approach to create strong adhesion between carbon and cordierite, promoted by the introduction of –OH groups on both surfaces [163,164]. Electrostatic interactions between negatively charged CNFs and positively charged $–NH_2$ groups of a 3-aminopropyl-triethoxysilane functionalized silicon substrate have also been used to promote adhesion of a CNF film [165].

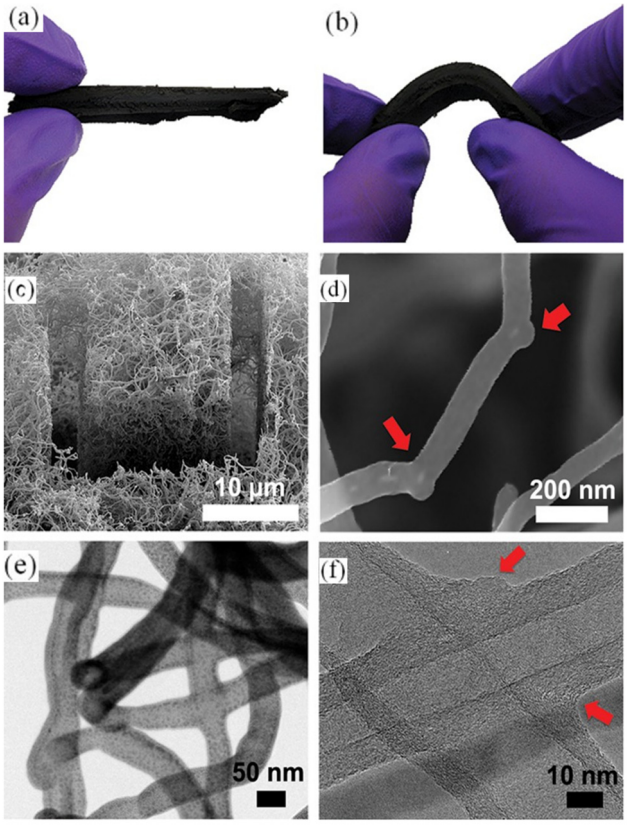

Figure 8. Physical structure and morphology of the CBxMWCNT (boron-doped MWCNT) 3-D network: (**a**) photograph of the 3D macroscopic CBxMWCNT solid sponge material as-produced; (**b**) photograph of the flexibility and mechanical stability upon bending the sample (**a**) by hand; (**c**) SEM image after ion beam "slice and view" feature, showing the interior porous structure of the entangled nanotube network; (**d**) closer look at the "elbow" defects found in the CBxMCWNT solids; (**e**) STEM image showing two, four-way covalent nanojunctions in series; (**f**) TEM image showing two overlapping CBxMCWNTs welded together, assisted by boron doping [125].

4.3. Preparation of Macro-Structures with Pre-Formed CNF

4.3.1. Vacuum Filtration

Filtration of a pre-formed CNF suspension through a filter or membrane, commonly known as buckypapers, is a well-established method used in the formation of free-standing CNF films; for instance, when carbon nanotubes are used [154,166]. Filtering is carried out using a CNF suspension through a commercial filter or membrane. The porosity and thickness of the membrane can be adjusted depending on the target CNF's film characteristics. The filtering speed has also been shown to affect the formation of the film; reports on slow [116] and quick [167] filtration to achieve homogeneous and stable films can be found in the literature. Often, the suspension preparation is found to have a more significant impact on the characteristics of the film than the fabrication process itself [168]. Alumina membranes are commonly used as the separation of the CNF film can be readily achieved by dissolution of the membrane in an acidic solution [153]. Mixed cellulose ester and acetate cellulose membranes and dissolvable filter papers, similarly, can be dissolved with acetone [169,170]. Simple peeling-off of a CNF film can also be achieved when using suitable membrane material, such as PVDF [136]. The porosity of the resulting CNF film can be controlled by adding fillers to form a composite membrane, or even using CNF as the filler in alternative membrane formulation, for example in graphene/CNF formulations [171,172]. Composite membranes are often also explored as a means to obtain hierarchal porosities combined with improved functionalities, for example combining CNF with

metallic nanoparticles [173,174]. Composite membranes can also be prepared by vacuum filtration of a CNF/polymer suspension/solution, e.g., CNF/PVDF, PEI, or PVP, followed by heat treatment of the resulting film to obtain the final composite membrane [175,176].

The same method is also used to prepare membranes coated with CNF, where the filtrating membrane serves as a support for the CNF layers, e.g., by filtration of a CNF suspension through a mixed cellulose ester membrane that is not removed post-filtering of the CNF [172]. Traditional ceramic, polymeric, carbon fiber, or other membranes can be used for this effect. Depending on the application and material, pre-treatment of the membranes to modify their texture (such as activation of carbon fiber membranes) or surface chemistry (doping with ligands to promote fixation of the CNFs) may be required. A number of different approaches are reported in the literature for this type of CNF-containing structures. Polysulfone ultrafiltration membranes have been functionalized with an amine reactive ester after being fixated onto carboxyl, carbonyl, and hydroxyl groups introduced on the membrane surface by O_2 plasma treatment. The functionalized membrane surface could then create cross-links with amine-functionalized CNF. Moreover, layer-by-layer deposition of intercalated positively and negatively charged CNFs, respectively functionalized with carboxyl or aminated groups, was carried out to increase the thickness of the CNF layer [177]. A bilayered membrane has also been prepared using CNFs layered on top of a macroporous silica substrate to obtain a membrane with controlled hierarchal porosity, with the thin CNF top-layer forming a rough surface due to the macroporosity of the silica substrate underneath [178]. Vacuum filtration has also been used to form composite membranes consisting of aligned hollow CNFs (e.g., carbon nanotubes) inside a polymeric matrix, where the hollow 1D carbon nanomaterials create the channels through the polymer matrix that allow for membrane separation [179,180].

4.3.2. Deposition Coating

CNF suspensions can also be used to form layers on top of 2D and 3D structures, either by solvent-drying or by promoting interactions between materials in suspension and the substrate.

Simple drying of a water-based CNF suspension has been used to prepare films on electrode surfaces [181]. The CNFs were pre-treated with HNO_3 to introduce acid surface groups that improve their dispersion in water. The suspension pH was set to 1 to raise the limit of suspension of the CNFs to 5 mg·mL^{-1} without precipitation. The films were obtained by drying a drop of the suspension on the electrode and repeating the process twice to obtain a uniform coating on the electrode surface. A similar method has been reported to prepare a CNF-covered glassy carbon electrode by evaporation of a 5% Nafion solution to form a thin catalytic layer for methanol oxidation [182], and as Pt support for oxygen reduction [183]. Air electrodes containing CNFs for rechargeable Li–air batteries have also been prepared by filtering of a DMF-based suspension to form free-standing α-MnO_2/CNF composite papers [184]. Another work found that more homogeneous films could be obtained by layer-by-layer deposition of a DMF suspension rather than a one-step deposition when preparing films for bioelectrodes [89]. Grafting of CNF from an ethanol dispersion has been used to prepare a polyurethane (PU) membrane for oil–water separation [185]. Ethanol is used as the dispersion medium so as to avoid hydrophobic interactions that promote agglomeration of the CNFs; likewise, ultrasonic processing was carried out to ensure good dispersion of the materials. A simple dip-coating method was then used to coat the membrane's available surface, including within the PU large pores. This resulted in a PU/CNF composite with increased surface area and reduced pore size able to successfully and efficiently separate oil from water. Knife casting has also been used as a technique to prepare mixed matrix membranes using CNF dispersed in a polysulfone matrix [186]. The dispersion of CNF in the membrane matrix was aided by a two-step functionalization of the carbon material by introduction of oxygen-containing surface groups by oxidation with a sulfuric and nitric acid mixture, and by introduction of aminated surface groups using ethylenediamine as a precursor. The amine groups were simultaneously used to increase selectivity in CO_2 from CH_4 as well as N_2 from O_2 separation. Precipitation of a CNF isopropanol dispersion using Nafion as an ionomer to aid dispersion

on the carbon cloth has also been carried out in the preparation of a porous carbon nanofiber anode in direct methanol fuel cells [187].

Cordierite and SiC foam 3D macro-structured supports have also been coated with CNF through dip-coating [188,189]. The most common methodology relies on the use of polymeric binders to adhere the CNF layers to the macro-structured support, and to maintain the structural integrity of the coated layer by promoting inter-particle binding [190]. More recently, formation of stable CNF suspensions by a combination of mechanical processing and chemical functionalization showed that stable nanostructured layers could be designed without a polymeric binder, where stability was directly linked with the deagglomeration of bundles in suspension [140]. Coating of such macro-porous supports is aided by capillary forces absorbing the suspension towards the support surface. Dip-coating provides a platform for control of film structure and thickness, by controlling factors such as dipping time, number of iterations, and concentration and viscosity of the suspension [191]. The latter can be adjusted through control of the CNF concentration, use of rheology modifiers, and by the morphology of the CNF particles and bundles themselves [140].

Electrophoretic deposition was used to achieve a coating of CNF/glassy carbon electrodes. CNF were dispersed in ethanol with $Mg(NO_3)\cdot 6H_2O$ to positively charge the suspended fibers [83]. The deposition was carried out by generating a 30 V potential between two electrodes immersed in the suspension, forming a thin 743 $\mu g \cdot cm^{-2}$ film on the electrode surface by promoting the aggregation of the nanomaterials towards the electrode by inducing their electromobility. A similar method has been used to form stable CNF coatings on metallic substrates, where improved adhesion was found to be obtained by bonding of acidic groups introduced on the surface of the carbon with metal hydroxides formed during the process on the metallic substrate/electrode surface [192]. Ionic strength-induced electrochemical deposition, using low voltages, has also been used to form CNF coatings; this method relies on the control of the ionic strength near the electrode surfaces, promoting the formation of coatings due to the decrease in the electrical double layer (EDL) interparticle repulsion with increasing ionic strength [193].

4.3.3. Spray-Coating

Spray techniques (sometimes referred to as air-brushing) have also been widely used to form CNF coatings on a variety of substrates, and even to form 3D structures. The technique relies again on the formation of a stable suspension using the approaches already described in detail. The suspensions are fed onto a spraying nozzle either by a compressed gas flow or alternatively using a syringe plunger [194]. The spraying aerosol is formed through the pressure of the carried liquid passing through the nozzle when using compressed gas, by using an ultrasonic transducer in a pre-nozzle chamber to form airborne droplets [194], or by creating an electrical potential between the nozzle and the substrate (electrospray assisted deposition) [195].

Spraying has been used to fabricate circular electrodes using an aluminum mask to shape the circular pattern of the electrodes. The DMF-based CNF suspensions were sprayed onto the substrates heated above the boiling point of the solvent to evaporate it upon contact, avoid the "coffee ring" effect where CNFs are pushed to the edges of the coated area (Figure 9) [196]. Patterning of similar CNF electrodes can also be achieved by post-spraying techniques, such as oxygen-plasma treatment [197]. The substrates can also be coupled to a moveable base support that facilitates covering of larger surface areas [198], or rotating setups to ensure homogeneous distribution of the coating [195]. Spraying can also be used to coat non-flat surfaces, such as fibers [199]. Nevertheless, this method is mostly limited by line-of-sight of the spray, except for electrospray-assisted deposition, which can take advantage of the potential between the nozzle and 3D substrates to promote formation of layers in areas inaccessible to straight-forward spray-coating [200].

The spraying method can be used to form coatings with a controlled number of layers or thickness by controlling the concentration of material in the spraying suspension or the spraying time to optimize the coating composition [201]. The layering effect was demonstrated to be best achieved by allowing

evaporation of the solvent between spraying of each layer [202]. This method has also been used to form coatings with pre-formed CNF composites, including metallic nanoparticles [202].

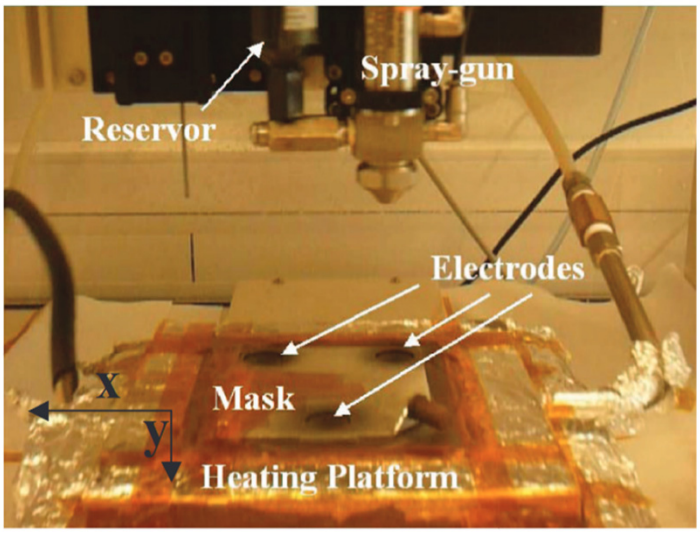

Figure 9. Experimental setup used for the spraying of CNF electrodes on graphite paper collectors with the use of an aluminum mask for circular pattern shaping and a heated substrate to evaporate solvents upon contact [196].

Spray-coating has been combined with dip-coating on PET substrates to form interlinked networked films as the spray coated material forms bridges between the coated material, resulting in increased percolation and consequently improved electrical conductivity [193].

Layer-by-layer ultrasonic spray-coating of CNF using radical initiated cross-linking of the individual particles has been used to achieve formation of 3D chemically cross-linked foam-like macro-structures [149].

CNF have also been mixed with metallic oxides to form composite coatings by spray-coating [193]. Spray-drying was firstly used to create the metallic/CNF mixtures, which were then sprayed onto the substrates. Interestingly, the abrasion caused by the metallic oxide particles during spraying was found to affect the morphology of the CNF, often leading to shorter lengths. Planetary ball-milling has also been used to obtain sprayable oxide/CNF mixtures [203].

4.3.4. Spin-Coating

Spin-coating consists of the use of centrifugal forces to spread a suspension over a flat substrate to obtain uniform coatings. Similar to vacuum filtration, this method has been used to form CNF coatings and free-standing films, depending on the nature and post-processing of the substrate layer [204]. The preparation of the CNF suspension is, as for the other techniques detailed here, essential for obtaining quality uniform films [205,206]. Unlike with spray-coating, since using a heated substrate is impractical, the choice of solvent often tends towards volatile organic solvents, such as dichloroethane (DCE) [207].

This method has been used to form CNF electrodes with high density networks due to the absence of charge repulsions between CNF/surfactant complexes when using a non-ionic surfactant [204]. The method has also been successfully used using CNF/polymer composites, where it was suggested that the viscosity of the suspensions hindered agglomeration up to an upper shear force limit and CNF concentration [208]. As with spray-coating, spin-coating can be used to form coatings with pre-formed CNF composites, for example using CNF/metallic oxide particles mixtures [209]. Metallic oxide/CNF composite films have also been obtained by spinning a suspension of CNFs with organometallic precursors, which were thermally treated post-deposition to form the respective metallic oxide composites [210]. Similarly, spin-coating has been used with polymer/CNF composites [211].

The uniformity of the obtained films using PMMA was found to be dependent on the carbon concentration in the spinning suspension [212]. The thickness and quality of such films can be easily controlled by the spinning parameters [213].

4.3.5. Printing

Screen-printing consists of the transfer of a suspension (or ink) through a mesh onto a target substrate, generally using a blade to force the ink through the mesh. For this end, high-content paste is generally used as higher viscosity is required for the technique, which can be achieved by adding additional additives to the CNF mixture [214]. The method is scalable and has a high-throughput as it can be applied to large areas at once.

Despite the requirements for forming a paste-like suspension, the dispersion of the CNF is still a critical factor and requires chemical and/or mechanical processing [215]. The thickness of the films can be controlled by either the CNF paste content or the number of layers printed onto the substrate [216]. This methodology can also be used to directly print CNF-containing composites such as sol-gel prepared composites of TiO_2 [217] and for polymer-based composites [218].

Inkjet printing has also been used to prepare CNF films, and is particularly used for application where patterning is required for the process. The technique relies on the inclusion of a CNF-containing ink into the already well-established inkjet printing technique [219]. As for other techniques based on CNF suspensions, the carbon material dispersion and characteristics of the ink are crucial to obtain good quality films using inkjet printing. Specifically for this method, low surface tension is required due to the low amount of ink being dispensed by the nozzle; organic solvents already have a low enough surface tension, but water-based suspensions require modification with wetting agents to achieve the necessary surface tension [219]. The inkjet printing technique is also very sensitive to the "coffee ring" effect; modification of the CNF [220], and substrate modification and heating [221], have tbeen used to maintain the uniformity of the printed films.

Similar to other printing and coating techniques, the structure of the coating can be controlled by changing the ink formulation and the number of prepared layers [219]. Similarly, the bridging of the individual CNF can be achieved by printing enough layers to form percolating, interconnected networks [222]. The addition of polymers to the ink formulation and control of the droplet ejection velocity have both been demonstrated to be able to achieve more uniform CNF films [220]. As for other CNF-suspension based techniques, composite films can easily be fabricated by using pre-formed mixtures [223].

CNF macro-structures have also been prepared by 3D printing/additive manufacturing. 3D printing is a recently popularized technique with different versions (robocasting, fused deposition modelling, etc.); the most common/popular version relies on the sequential deposition of layers of material to form a macro-structure [224]. The technique has the potential to be integrated into a digitally controlled manufacturing process as designs can be translated directly from CAD-type applications, either for prototyping or manufacturing. In particular, its application in chemical engineering has been explored to produce reactors with complex shapes and even catalytically active reactorware, with control even at very small scales (Figure 10) [224].

CNFs have been tested extensively as fillers incorporated onto polymer-based inks (e.g., epoxy) to improve their mechanical properties [226]; this was carried on from other traditional methods to prepare polymeric macro-structures and is widely explored within the field of structural engineering [157]. The challenge for CNF-containing, chemically active, 3D-printed macro-structures is the preparation of inks that retain the mechanical robustness of the CNF-filled polymer formulations, while providing access for the reactants to the CNF to take advantage of their chemical properties [227]. Unlike other techniques discussed here, 3D printing of CNF-containing, chemically active structures is not as well developed. The most common techniques for ink preparation, however, follow closely what is here detailed for other types of techniques. The methods detailed here to improve robustness of free-standing CNF structures are also likely to gain relevance in the design of chemically active 3D structures.

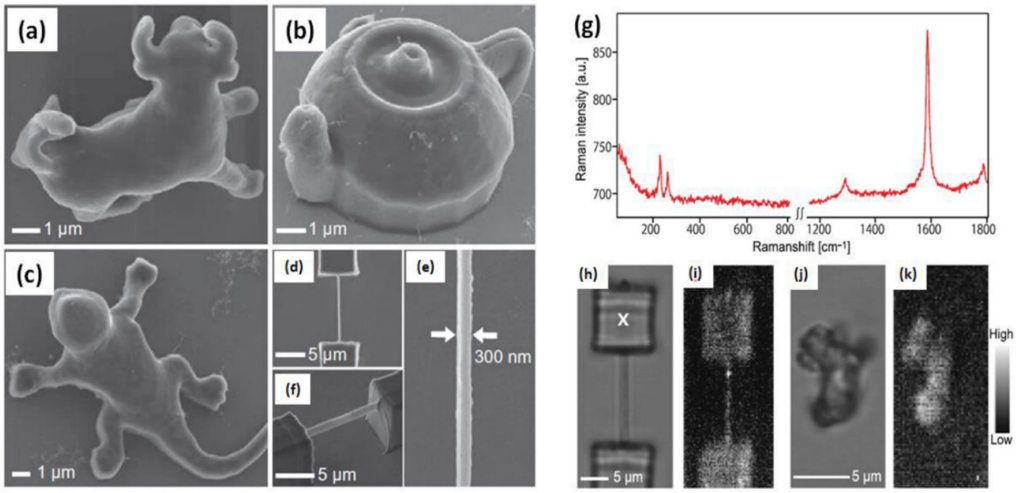

Figure 10. 3D micro/nano structural SWCNT/polymer composites are fabricated by using the TPP lithography. The structures in (**a**–**f**) are an 8-μm-long micro bull, a micro tea pod, a micro lizard, a nanowire suspended between two micro boxes, magnified image of (**d**), and perspective view of the nanowire, respectively; (**g**) shows a Raman spectrum taken from the box suspending the nanowire with an excitation wavelength of 785 nm. Laser power and exposure time are 2.8 mW and 60 s, respectively; (**h**) a bright field image of the 300-nm-thick nanowire suspended between two boxes; (**i**) a G-band Raman image taken at the same area in (**h**). Laser power and exposure time are 1.4 mW and 10 s, respectively; (**j**) a bright field image of an 8-μm-long micro bull; (**k**) a G-band Raman image taken at the same area in (**h**). Laser power and exposure time are 2.8 mW and 10 s, respectively [225].

Nevertheless, examples are available in the literature for CNF-containing 3D structures. CNFs have been introduced into stereolithography-printed PEGDA scaffolds to modify their surface properties through creation of nanofeatures and induce electrical conductivity to enhance the interaction between neural cells and biomaterials [228]. CNFs have also been introduced onto extrusion-printed PIC hydrogel scaffolds with improved compatibility in bone regeneration procedures [229]. Liquid deposition modelling was used to also fabricate CNF/PLA composite conductive macro-structures, where an increase in the electrical conductivity of the printed matrix increased with the increase in CNF, at the cost of its structural robustness [230]. Ionic liquids have been used in CNF/PMMA formulations as a plasticizer and CNF functionalization to obtain 3D-printed structures with high conductivity and good mechanical robustness (Figure 11) [231]. Adaptations to the printing setups have been shown to aid in the formation of CNF-containing micro-structures by, e.g., improving solvent evaporation [232].

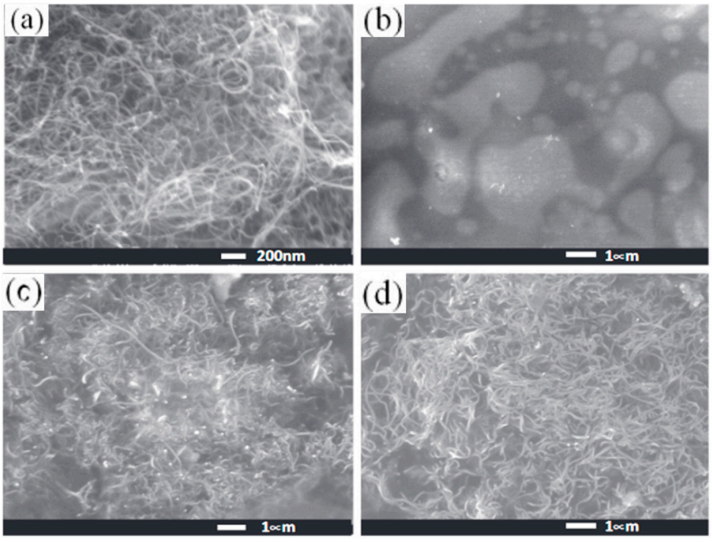

Figure 11. *Cont.*

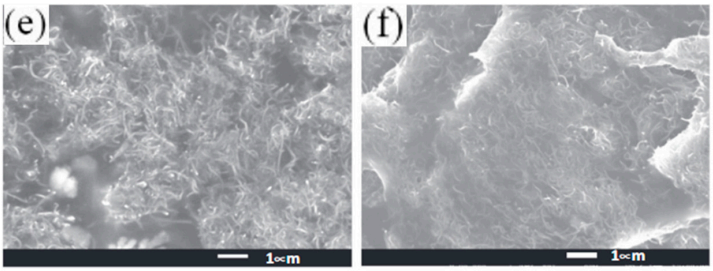

Figure 11. (**a**) Pristine CNF (multi-walled carbon nanotubes) and (**b**) PIL-PMMA-IL composite and nanocomposites; (**c**) MWCNT 5 wt.%, IL45; (**d**) MWCNT 8 wt.%, IL42; (**e**) MWCNT 15 wt.%, IL35; and (**f**) cross-section of a filament with MWCNT 8 wt.%, IL42 [231].

5. Catalytic Applications

The techniques detailed above are all suitable for application in the preparation of catalytic CNF-containing macro-structures, with several examples available in the relevant literature. This section highlights specific examples using a selection of the techniques discussed in the previous sections.

Electrospinning has been reportedly used to prepare Ni-decorated CNF membranes that showed high catalytic activity in a hydrogen evolution reaction (HER) [233]. The PAN-based membranes showed improved electrocatalytic activity upon Ni deposition, as the larger interfacial area between the carbon nanofibers and Ni nanoparticles leads to higher apparent current density at a specified overpotential (Figure 12).

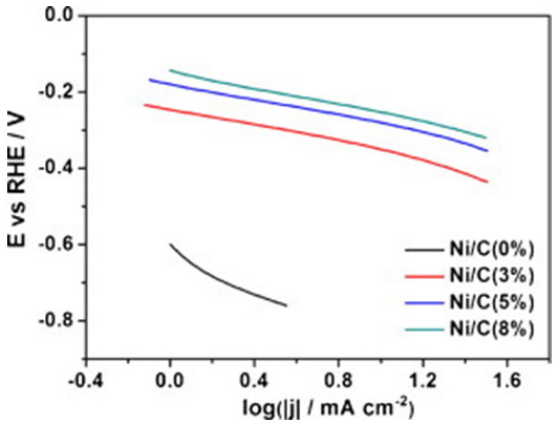

Figure 12. Tafel plots for Ni-decorated carbon nanofibers [233].

Chemical vapor deposition of CNFs on macro-structured supports by decomposition of a gaseous carbon source has been used to prepare catalysts for liquid-phase ozonation of organic pollutants [43]. Ethane was decomposed over Ni nanoparticles dispersed over an alumina layer on a cordierite macro-structured support to obtain a dense layer of CNF. Ammonia was introduced to obtain N-doped CNF; N-doped carbon is a more active catalyst for ozonation of water-based organic pollutants due to the enhanced availability of delocalized π-electrons on the carbon surface. However, ammonia hinders the formation of the CNF layer, resulting in a reduced yield of catalytic material. Thus, the final macro-structured catalysts with nitrogen are more active per mass of catalytic material, but less efficient overall in the ozonation process (Figure 13).

Vacuum filtration has been used to prepare CNF-containing membranes supported on PTFE membranes, where the CNFs were previously modified with nitric acid and/or gold nanoclusters [234]. The synthesized gold nanocluster/CNF membrane was found to be efficient in the reduction of 4-nitrophenol in a continuous flow reactor, achieving complete removal of the pollutant even at very short contact times (3.0 s, Figure 14).

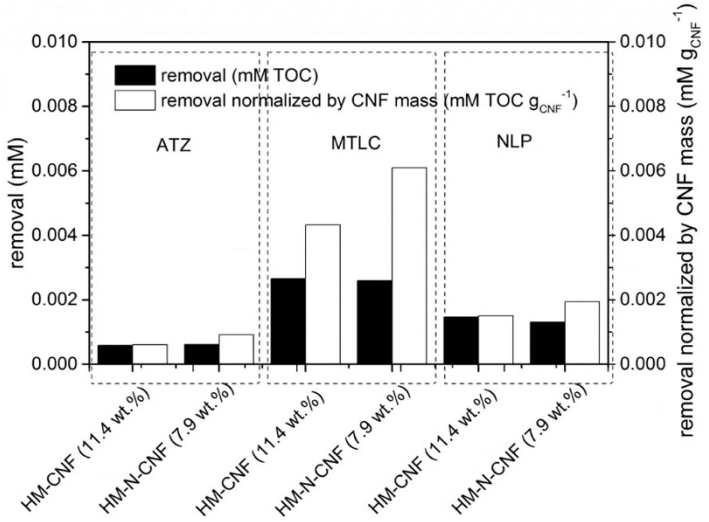

Figure 13. Removal of TOC at steady state during continuous ozonation experiments of atrazine (ATZ, C_{inlet} = 0.046 mM), metolachlor (MTLC, C_{inlet} = 0.070 mM), and nonylphenol (NLP, C_{inlet} = 0.027 mM), using unmodified and N-doped CNF-covered monoliths [43].

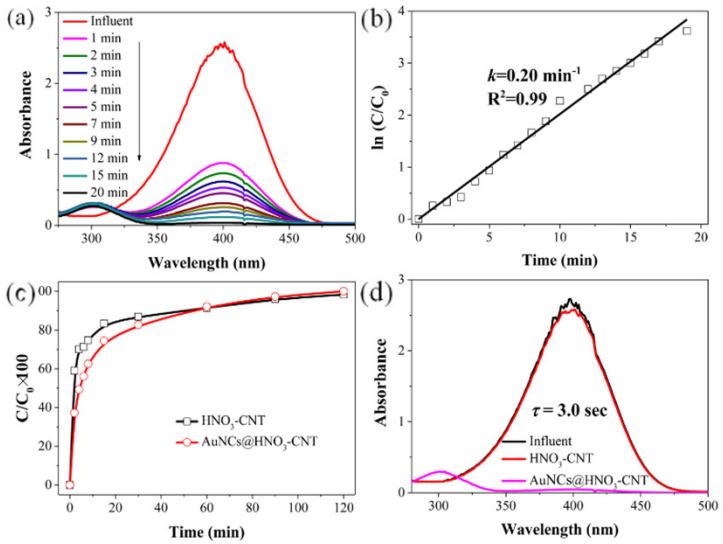

Figure 14. (**a**) Time-dependent UV–vis absorption spectra from 280 to 500 nm and (**b**) the rate kinetics for the conversion of 4-NP in a conventional batch reactor using the AuNCs/CNTs hybrid membrane. (**c**) Breakthrough curves of 4-NP only (without the addition of any $NaBH_4$; the data was obtained at the wavelength of 317 nm). (**d**) Comparison of the UV–vis absorption spectra before and after passing through the AuNCs/CNTs hybrid membrane and the HNO_3-CNTs membrane [234].

Dip-coating is widely used to prepare macro-structured catalysts for environmental applications, namely those used in the automotive industry, normally based on mixed oxides with or without precious metals as catalysts. Examples of dip-coating with CNF for catalytic applications are not as common; however, this technique has been used to prepare macro-structured SiC foam catalysts, which have been shown to retain some activity when compared with the powder-form counterparts in the hydrogenation of nitrobenzene [188]. However, the use of a binder was found to significantly reduce the activity of the catalysts (Figure 15).

Spray-coating has also been used to prepare CNF coatings with catalytic activity. The inclusion of CNF on a TiO_2 coating prepared by spraying onto a substrate was found to improve the photocatalytic activity of the composite when compared with the TiO_2 coating alone [235]. The composite powder was prepared by growth of CNFs directly on the titania particles before preparation of the coating

by spraying. The coated film was found to be less active when compared with the powder material, but the composite coating compared favorably with the titania-only coating (Figure 16).

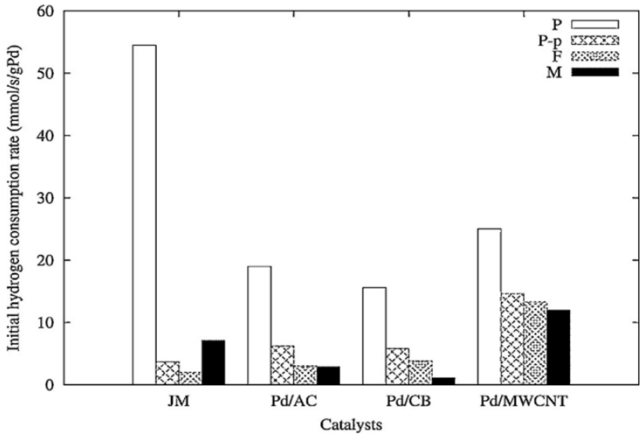

Figure 15. Initial hydrogen consumption rates during nitrobenzene hydrogenation (3 bars, 40 °C) for the different catalysts. P refers to the initial powder, P-p to the scrapped powder, F to the coated foam, and M to the crushed coated monolith [188].

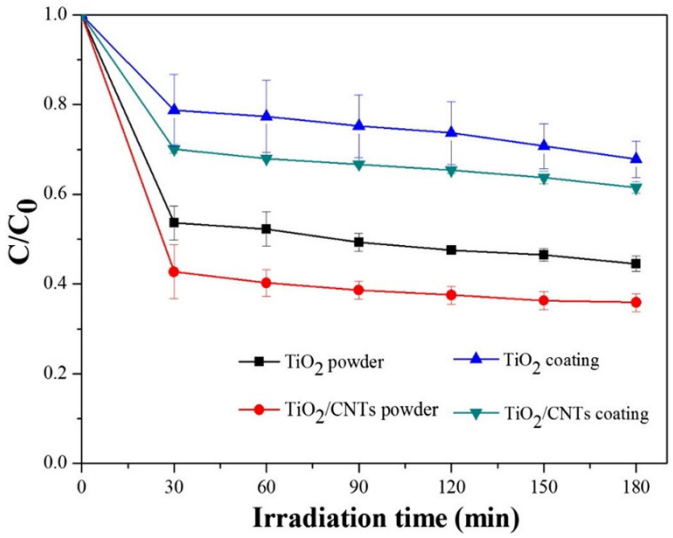

Figure 16. Comparison of photocatalytic decay of methylene blue for the rutile-TiO_2 powder, TiO_2/CNTs composite powders, TiO_2 coating, and TiO_2/CNTs composite coating under UV light irradiation at 120 min [235].

Some of the discussed techniques have been extensively described in the literature to prepare CNF-containing catalytic macro-structures, namely, electrospinning, vacuum filtration, or chemical vapor deposition. Opportunities exist for the application of other techniques to prepare catalytic macro-structures, as described in the next section.

6. Future Outlooks and Concluding Remarks

The preparation of CNF-containing macrostructures is an already well-developed field, with the techniques more heavily researched in the last few years now benefiting from a very comprehensive understanding of the chemistry and physics behind it. However, it is clear that most techniques have yet to be intensively applied in the fabrication of catalytic structures; in fact, the better developed fields seem to be in the electrochemistry-related areas, such as field emission displays, materials for fuel cells, or sensors. On the other hand, there is already enough knowledge available to further increase the research of structured CNF catalysts, in particular for ex situ fabrication methods. These have

the potential to take advantage of the powder-processing methods, shown to enhance the catalytic performance of CNFs and translate these onto macro-structured catalysts.

Hence, the following opportunities are suggested for future research in the field of catalytic CNF macrostructures that are available to the research community:

- improved robustness of electrospinning-prepared CNF structures;
- development of alloyed metallic catalysts for low-cost synthesis of CNF films by CVD;
- large-scale and high-throughput fabrication methods for structures prepared by spin- and spray-coating;
- new CNF formulations for printing to find compromises between CNF surface availability for catalytic reactions and mechanical robustness, in particular for novel 3D printing applications.

7. Conclusions

A review of methods reported for the fabrication of carbon nanofibers (CNFs) in the form of macrostructures is presented here. The incentives for use of CNFs as catalysts or catalyst supports in a variety of reactions are discussed, and linked to the particular chemical, textural, and morphological properties of CNFs. The reasons for the development of methodologies for preparation of CNF macro-structures is also discussed, and it is proposed that the macro-structuring of CNFs is required due to difficulties in the handling of nanosized powders in traditional packed-bed reactors and other similar configurations, and concerns regarding the release of nanoparticles in harsher operation conditions.

The macro-structure preparation methodologies are divided based on whether the preparation method directly results in a macrostructure (electrospinning and chemical vapor deposition), or whether pre-synthesized CNFs are used to form new macro-structures (coating and printing techniques). Advantages and drawbacks of both approaches are detailed, in particular concerning the ease of scaling-up, stability, and catalytic activity.

The review also identifies future avenues for research in the topic, in particular in the translation of the described methodologies to catalytic applications, and in the requirements for less well-explored techniques to be effective in the preparation of structured catalysts. Suitable techniques for the preparation of CNF macro-structures, with potential for use as catalysts but with little expression in this area currently, are identified; one particular highlight is the use of additive manufacturing (or 3D printing) using CNFs to simultaneously improve the mechanical properties of 3D-printed macro-structures and providing these with intrinsic catalytic activity.

Author Contributions: Conceptualization, J.R. and O.S.G.P.S.; writing—original draft preparation, J.R.; writing—review and editing, J.R., O.S.G.P.S. and M.F.R.P.; supervision, O.S.G.P.S. and M.F.R.P.; funding acquisition, O.S.G.P.S. and M.F.R.P. All authors have read and agreed to the published version of the manuscript.

Funding: InTreat-PTDC/EAM-AMB/31337/2017—POCI-01-0145-FEDER-031337-funded by FEDER funds through COMPETE2020-Programa Operacional Competitividade e Internacionalização (POCI) and by national funds (PIDDAC) through FCT/MCTES; NanoCatRed—NORTE-01-0247-FEDER-045925-co-financed by the ERDF—European Regional Development Fund through the Operation Program for Competitiveness and Internationalization—COMPETE 2020, and the North Portugal Regional Operational Program—NORTE 2020 and by the Portuguese Foundation for Science and Technology—FCT under UT Austin Portugal. Associate Laboratory LSRE-LCM-UID/EQU/50020/2019-funded by national funds through FCT/MCTES (PIDDAC). OSGPS acknowledges FCT funding under the Scientific Employment Stimulus—Institutional Call.

Acknowledgments: All figures re-printed with permission from respective owners.

Conflicts of Interest: The authors declare no conflict of interest.

References

1. Louis, B.; Bégin, D.; Ledoux, M.J.; Pham-Huu, C. Advances in the Use of Carbon Nanomaterials in Catalysis. In *Ordered Porous Solids*; Elsevier: Amsterdam, The Netherlands, 2009; pp. 621–649.
2. Hiremath, N.; Bhat, G. High-performance carbon nanofibers and nanotubes. In *Structure and Properties of High-Performance Fibers*; Elsevier Inc.: Amsterdam, The Netherlands, 2017; pp. 79–109.

3. Martin-Gullon, I.; Vera, J.; Conesa, J.A.; González, J.L.; Merino, C. Differences between carbon nanofibers produced using Fe and Ni catalysts in a floating catalyst reactor. *Carbon* **2006**, *44*, 1572–1580. [CrossRef]
4. Van Dommelle, S. Nitrogen Doped Carbon Nanotubes: Synthesis, Characterization and Catalysis. Ph.D. Thesis, Utrecht University, Utrecht, The Netherlands, 2008.
5. Shu, G.J.; Liou, S.C.; Karna, S.; Sankar, R.; Hayashi, M.; Chu, M.W.; Chou, F.C. Graphene-like conjugated π bond system in Pb1-xSnxSe. *Appl. Phys. Lett.* **2015**, *106*, 122101. [CrossRef]
6. Serp, P.; Machado, B. *Nanostructured Carbon Materials for Catalysis*; The Royal Society of Chemistry: London, UK, 2015.
7. Figueiredo, J.L.; Pereira, M.F.R.; Freitas, M.M.A.; Órfão, J.J.M. Modification of the surface chemistry of activated carbons. *Carbon* **1999**, *37*, 1379–1389. [CrossRef]
8. Cabiac, A.; Cacciaguerra, T.; Trens, P.; Durand, R.; Delahay, G.; Medevielle, A.; Plée, D.; Coq, B. Influence of textural properties of activated carbons on Pd/carbon catalysts synthesis for cinnamaldehyde hydrogenation. *Appl. Catal. A Gen.* **2008**, *340*, 229–235. [CrossRef]
9. Amadou, J.; Chizari, K.; Houllé, M.; Janowska, I.; Ersen, O.; Bégin, D.; Pham-Huu, C. N-doped carbon nanotubes for liquid-phase CC bond hydrogenation. *Catal. Today* **2008**, *138*, 62–68. [CrossRef]
10. Solhy, A.; Machado, B.F.; Beausoleil, J.; Kihn, Y.; Gonçalves, F.; Pereira, M.F.R.; Órfão, J.J.M.; Figueiredo, J.L.; Faria, J.L.; Serp, P. MWCNT activation and its influence on the catalytic performance of Pt/MWCNT catalysts for selective hydrogenation. *Carbon* **2008**, *46*, 1194–1207. [CrossRef]
11. Farzadkia, M.; Shahamat, Y.D.; Nasseri, S.; Mahvi, A.H.; Gholami, M.; Shahryari, A. Catalytic Ozonation of Phenolic Wastewater: Identification and Toxicity of Intermediates. *J. Eng.* **2014**, *2014*, 520929. [CrossRef]
12. Yang, S.; Li, X.; Zhu, W.; Wang, J.; Descorme, C. Catalytic activity, stability and structure of multi-walled carbon nanotubes in the wet air oxidation of phenol. *Carbon* **2008**, *46*, 445–452. [CrossRef]
13. Wepasnick, K.A.; Smith, B.A.; Schrote, K.E.; Wilson, H.K.; Diegelmann, S.R.; Fairbrother, D.H. Surface and structural characterization of multi-walled carbon nanotubes following different oxidative treatments. *Carbon* **2011**, *49*, 24–36. [CrossRef]
14. Vanyorek, L.; Meszaros, R.; Barany, S. Surface and electrosurface characterization of surface-oxidized multi-walled N-doped carbon nanotubes. *Colloids Surf. A Physicochem. Eng. Asp.* **2014**, *448*, 140–146. [CrossRef]
15. Serp, P.; Figueiredo, J.L. (Eds.) *Carbon Materials for Catalysis*; John Wiley & Sons, Inc.: Hoboken, NJ, USA, 2008.
16. *IUPAC Compendium of Chemical Terminology*; Wiley-Blackwell: Hoboken, NJ, USA, 2009.
17. Thakur, D.B.; Tiggelaar, R.M.; Gardeniers, J.G.E.; Lefferts, L.; Seshan, K. Silicon based microreactors for catalytic reduction in aqueous phase: Use of carbon nanofiber supported palladium catalyst. *Chem. Eng. J.* **2013**, *227*, 128–136. [CrossRef]
18. Donaldson, K.; Poland, C.A.; Murphy, F.A.; MacFarlane, M.; Chernova, T.; Schinwald, A. Pulmonary toxicity of carbon nanotubes and asbestos—Similarities and differences. *Adv. Drug Deliv. Rev.* **2013**, *65*, 2078–2086. [CrossRef] [PubMed]
19. Toyokuni, S. Genotoxicity and carcinogenicity risk of carbon nanotubes. *Adv. Drug Deliv. Rev.* **2013**, *65*, 2098–2110. [CrossRef]
20. Shvedova, A.A.; Yanamala, N.; Kisin, E.R.; Tkach, A.V.; Murray, A.R.; Hubbs, A.; Chirila, M.M.; Keohavong, P.; Sycheva, L.P.; Kagan, V.E.; et al. Long-term effects of carbon containing engineered nanomaterials and asbestos in the lung: One year postexposure comparisons. *Am. J. Physiol. Lung Cell. Mol. Physiol.* **2014**, *306*, 172–182. [CrossRef]
21. Kisin, E.R.; Murray, A.R.; Keane, M.J.; Shi, X.C.; Schwegler-Berry, D.; Gorelik, O.; Arepalli, S.; Castranova, V.; Wallace, W.E.; Kagan, V.E.; et al. Single-walled carbon nanotubes: Geno- and cytotoxic effects in lung fibroblast V79 cells. *J. Toxicol. Environ. Health Part A Curr. Issues* **2007**, *70*, 2071–2079. [CrossRef]
22. Murray, A.R.; Kisin, E.R.; Tkach, A.V.; Yanamala, N.; Mercer, R.; Young, S.H.; Fadeel, B.; Kagan, V.E.; Shvedova, A.A. Factoring-in agglomeration of carbon nanotubes and nanofibers for better prediction of their toxicity versus asbestos. *Part. Fibre Toxicol.* **2012**, *9*, 10–29. [CrossRef]
23. Kisin, E.R.; Murray, A.R.; Sargent, L.; Lowry, D.; Chirila, M.; Siegrist, K.J.; Schwegler-Berry, D.; Leonard, S.; Castranova, V.; Fadeel, B.; et al. Genotoxicity of carbon nanofibers: Are they potentially more or less dangerous than carbon nanotubes or asbestos? *Toxicol. Appl. Pharmacol.* **2011**, *252*, 1–10. [CrossRef]
24. Gonçalves, A.G.; Figueiredo, J.L.; Órfão, J.J.M.; Pereira, M.F.R. Influence of the surface chemistry of multi-walled carbon nanotubes on their activity as ozonation catalysts. *Carbon* **2010**, *48*, 4369–4381. [CrossRef]

25. Rocha, R.P.; Silva, A.M.T.; Romero, S.M.M.; Pereira, M.F.R.; Figueiredo, J.L. The role of O- and S-containing surface groups on carbon nanotubes for the elimination of organic pollutants by catalytic wet air oxidation. *Appl. Catal. B Environ.* **2014**, *147*, 314–321. [CrossRef]
26. Liang, Y.; Zhang, H.; Yi, B.; Zhang, Z.; Tan, Z. Preparation and characterization of multi-walled carbon nanotubes supported PtRu catalysts for proton exchange membrane fuel cells. *Carbon* **2005**, *43*, 3144–3152. [CrossRef]
27. Guha, A.; Lu, W.; Zawodzinski, T.A.; Schiraldi, D.A. Surface-modified carbons as platinum catalyst support for PEM fuel cells. *Carbon* **2007**, *45*, 1506–1517. [CrossRef]
28. Soares, O.S.G.P.; Órfão, J.J.M.; Pereira, M.F.R. Nitrate reduction in water catalysed by Pd–Cu on different supports. *Desalination* **2011**, *279*, 367–374. [CrossRef]
29. Li, C.-H.; Yu, Z.-X.; Yao, K.-F.; Ji, S.; Liang, J. Nitrobenzene hydrogenation with carbon nanotube-supported platinum catalyst under mild conditions. *J. Mol. Catal. A Chem.* **2005**, *226*, 101–105. [CrossRef]
30. Chen, P.; Yang, F.; Kostka, A.; Xia, W. Interaction of cobalt nanoparticles with oxygen- and nitrogen-functionalized carbon nanotubes and impact on nitrobenzene hydrogenation catalysis. *ACS Catal.* **2014**, *4*, 1478–1486.
31. Chen, J.; Chen, Q.; Ma, Q. Influence of surface functionalization via chemical oxidation on the properties of carbon nanotubes. *J. Colloid Interface Sci.* **2012**, *370*, 32–38.
32. Toebes, M.L.; Prinsloo, F.F.; Bitter, J.H.; Van Dillen, A.J.; De Jong, K.P. Influence of oxygen-containing surface groups on the activity and selectivity of carbon nanofiber-supported ruthenium catalysts in the hydrogenation of cinnamaldehyde. *J. Catal.* **2003**, *214*, 78–87. [CrossRef]
33. Toebes, M.L. Support effects in hydrogenation of cinnamaldehyde over carbon nanofiber-supported platinum catalysts: Kinetic modeling. *Chem. Eng. Sci.* **2005**, *60*, 5682. [CrossRef]
34. Li, C.; Shao, Z.; Pang, M.; Williams, C.T.; Liang, C. Carbon nanotubes supported Pt catalysts for phenylacetylene hydrogenation: Effects of oxygen containing surface groups on Pt dispersion and catalytic performance. *Catal. Today* **2012**, *186*, 69–75. [CrossRef]
35. Fang, C.; Zhang, D.; Shi, L.; Gao, R.; Li, H.; Ye, L.; Zhang, J. Highly dispersed CeO_2 on carbon nanotubes for selective catalytic reduction of NO with NH_3. *Catal. Sci. Technol.* **2013**, *3*, 803–811. [CrossRef]
36. Chen, J.; Wang, M.; Liu, B.; Fan, Z.; Cui, K.; Kuang, Y. Platinum catalysts prepared with functional carbon nanotube defects and Its improved catalytic performance for methanol oxidation. *J. Phys. Chem. B* **2006**, *110*, 11775–11779. [CrossRef]
37. Rocha, R.P.; Santos, D.F.M.; Soares, O.S.M.P.; Silva, A.M.T.; Pereira, M.F.R.; Figueiredo, J.L. Metal-Free Catalytic Wet Oxidation: From Powder to Structured Catalyst Using N-Doped Carbon Nanotubes. *Top. Catal.* **2018**, *61*, 1957–1966. [CrossRef]
38. Figueiredo, J.L. Nanostructured porous carbons for electrochemical energy conversion and storage. *Surf. Coat. Technol.* **2018**, *350*, 307–312. [CrossRef]
39. Duan, X.; Sun, H.; Wang, Y.; Kang, J.; Wang, S. N-Doping-Induced Nonradical Reaction on Single-Walled Carbon Nanotubes for Catalytic Phenol Oxidation. *ACS Catal.* **2015**, *5*, 553–559. [CrossRef]
40. Ba, H.; Liu, Y.; Truong-Phuoc, L.; Duong-Viet, C.; Mu, X.; Doh, W.H.; Tran-Thanh, T.; Baaziz, W.; Nguyen-Dinh, L.; Nhut, J.-M.; et al. A highly N-doped carbon phase "dressing" of macroscopic supports for catalytic applications. *Chem. Commun.* **2015**, *51*, 14393–14396. [CrossRef]
41. Soares, O.S.G.P.; Rocha, R.P.; Gonçalves, A.G.; Figueiredo, J.L.; Órfão, J.J.M.; Pereira, M.F.R. Easy method to prepare N-doped carbon nanotubes by ball milling. *Carbon* **2015**, *91*, 114–121. [CrossRef]
42. Wong, W.Y.; Daud, W.R.W.; Mohamad, A.B.; Kadhum, A.A.H.; Loh, K.S.; Majlan, E.H. Recent progress in nitrogen-doped carbon and its composites as electrocatalysts for fuel cell applications. *Int. J. Hydrogen Energy* **2013**, *38*, 9370–9386. [CrossRef]
43. Restivo, J.; Garcia-Bordejé, E.; Órfão, J.J.M.; Pereira, M.F.R. Carbon nanofibers doped with nitrogen for the continuous catalytic ozonation of organic pollutants. *Chem. Eng. J.* **2016**, *293*, 102–111. [CrossRef]
44. Xu, X.; Jiang, S.; Hu, Z.; Liu, S. Nitrogen-Doped Carbon Nanotubes: High Electrocatalytic Activity toward the Oxidation of Hydrogen Peroxide and Its Application for Biosensing. *ACS Nano* **2010**, *4*, 4292–4298. [CrossRef]
45. Soares, O.S.G.P.; Rocha, R.P.; Órfão, J.J.M.; Pereira, M.F.R.; Figueiredo, J.L. Mechanothermal Approach for N-, S-, P-, and B-Doping of Carbon Nanotubes: Methodology and Catalytic Performance in Wet Air Oxidation. *C J. Carbon Res.* **2019**, *5*, 30. [CrossRef]

46. Gupta, R.; Sharma, S.C. Modelling the effects of nitrogen doping on the carbon nanofiber growth via catalytic plasma-enhanced chemical vapour deposition process. *Contrib. Plasma Phys.* **2019**, *59*, 72–85. [CrossRef]
47. Rocha, R.P.; Soares, O.S.G.P.; Gonçalves, A.G.; Órfão, J.J.M.; Pereira, M.F.R.; Figueiredo, J.L. Different methodologies for synthesis of nitrogen doped carbon nanotubes and their use in catalytic wet air oxidation. *Appl. Catal. A Gen.* **2017**, *548*, 62–70. [CrossRef]
48. Zhang, Y.; Zhang, J.; Su, D.S. Substitutional Doping of Carbon Nanotubes with Heteroatoms and Their Chemical Applications. *ChemSusChem* **2014**, *7*, 1240–1250. [CrossRef] [PubMed]
49. Li, X.-R.; Xu, J.-J.; Chen, H.-Y. Potassium-doped carbon nanotubes toward the direct electrochemistry of cholesterol oxidase and its application in highly sensitive cholesterol biosensor. *Electrochim. Acta* **2011**, *56*, 9378–9385. [CrossRef]
50. Gong, T.; Qi, R.; Liu, X.; Li, H.; Zhang, Y. N F-Codoped Microporous Carbon Nanofibers as Efficient Metal-Free Electrocatalysts for ORR. *Nano-Micro Lett.* **2019**, *11*, 9. [CrossRef]
51. Lee, Y.S.; Cho, T.H.; Lee, B.K.; Rho, J.S.; An, K.H.; Lee, Y.H. Surface properties of fluorinated single-walled carbon nanotubes. *J. Fluor. Chem.* **2003**, *120*, 99–104. [CrossRef]
52. Yuan, Z.; Peng, H.J.; Huang, J.Q.; Liu, X.Y.; Wang, D.W.; Cheng, X.B.; Zhang, Q. Hierarchical free-standing carbon-nanotube paper electrodes with ultrahigh sulfur-loading for lithium-sulfur batteries. *Adv. Funct. Mater.* **2014**, *24*, 6105–6112. [CrossRef]
53. Ummethala, R.; Fritzsche, M.; Jaumann, T.; Balach, J.; Oswald, S.; Nowak, R.; Sobczak, N.; Kaban, I.; Rümmeli, M.H.; Giebeler, L. Lightweight, free-standing 3D interconnected carbon nanotube foam as a flexible sulfur host for high performance lithium-sulfur battery cathodes. *Energy Storage Mater.* **2018**, *10*, 206–215. [CrossRef]
54. Restivo, J.; Rocha, R.P.; Silva, A.M.T.; Órfão, J.J.M.; Pereira, M.F.R.; Figueiredo, J.L. Catalytic performance of heteroatom-modified carbon nanotubes in advanced oxidation processes. *Cuihua Xuebao Chin. J. Catal.* **2014**, *35*, 896–905. [CrossRef]
55. Ania, C.O.; Armstrong, P.A.; Bandosz, T.J.; Beguin, F.; Carvalho, A.P.; Celzard, A.; Frackowiak, E.; Gilarranz, M.A.; László, K.; Matos, J.; et al. Engaging nanoporous carbons in "beyond adsorption" applications: Characterization, challenges and performance. *Carbon* **2020**, *164*, 69–84. [CrossRef]
56. Maldonado, S.; Stevenson, K.J. Influence of nitrogen doping on oxygen reduction electrocatalysis at carbon nanofiber electrodes. *J. Phys. Chem. B* **2005**, *109*, 4707–4716. [CrossRef]
57. Cheng, Y.; Fan, M.; Lin, W.; Zhang, Z.; Zhang, H. Platinum nanoparticles on defect-rich nitrogen-doped hollow carbon as an efficient electrocatalyst for hydrogen evolution reactions. *RSC Adv.* **2019**, *10*, 930–937. [CrossRef]
58. Pham-Huu, C. Carbon nanofiber supported palladium catalyst for liquid-phase reactions an active and selective catalyst for hydrogenation of cinnamaldehyde into hydrocinnamaldehyde. *J. Mol. Catal. A. Chem.* **2001**, *170*, 155–163. [CrossRef]
59. Rodriguez, N.M.; Kim, M.S.; Baker, R.T.K. Carbon nanofibers: A unique catalyst support medium. *J. Phys. Chem.* **1994**, *98*, 13108–13111. [CrossRef]
60. Tsuji, M.; Kubokawa, M.; Yano, R.; Miyamae, N.; Tsuji, T.; Jun, M.S.; Hong, S.; Lim, S.; Yoon, S.H.; Mochida, I. Fast preparation of PtRu catalysts supported on carbon nanofibers by the microwave-polyol method and their application to fuel cells. *Langmuir* **2007**, *23*, 387–390. [CrossRef] [PubMed]
61. Bezemer, G.L.; Radstake, P.B.; Koot, V.; Van Dillen, A.J.; Geus, J.W.; De Jong, K.P. Preparation of Fischer-Tropsch cobalt catalysts supported on carbon nanofibers and silica using homogeneous deposition-precipitation. *J. Catal.* **2006**, *237*, 291–302. [CrossRef]
62. Rodríguez, A.; Ovejero, G.; Romero, M.D.; Díaz, C.; Barreiro, M.; García, J. Catalytic wet air oxidation of textile industrial wastewater using metal supported on carbon nanofibers. *J. Supercrit. Fluids* **2008**, *46*, 163–172. [CrossRef]
63. Shaikhutdinov, S.K.; Avdeeva, L.B.; Novgorodov, B.N.; Zaikovskii, V.I.; Kochubey, D.I. Nickel catalysts supported on carbon nanofibers: Structure and activity in methane decomposition. *Catal. Lett.* **1997**, *47*, 35–42. [CrossRef]
64. Motoyama, Y.; Takasaki, M.; Yoon, S.H.; Mochida, I.; Nagashima, H. Rhodium nanoparticles supported on carbon nanofibers as an arene hydrogénation catalyst highly tolerant to a coexisting epoxido group. *Org. Lett.* **2009**, *11*, 5042–5045. [CrossRef]

65. Zhu, J.; Jia, Y.; Li, M.; Lu, M.; Zhu, J. Carbon Nanofibers Grown on Anatase Washcoated Cordierite Monolith and Its Supported Palladium Catalyst for Cinnamaldehyde Hydrogenation. *Ind. Eng. Chem. Res.* **2013**, *52*, 1224–1233. [CrossRef]
66. Zhang, P.; Jiang, F.; Chen, H. Enhanced catalytic hydrogenation of aqueous bromate over Pd/mesoporous carbon nitride. *Chem. Eng. J.* **2013**, *234*, 195–202. [CrossRef]
67. Williams, J.L. Monolith structures, materials, properties and uses. *Catal. Today* **2001**, *69*, 3–9. [CrossRef]
68. Salomons, S.; Hayes, R.E.; Votsmeier, M.; Drochner, A.; Vogel, H.; Malmberg, S.; Gieshoff, J. On the use of mechanistic CO oxidation models with a platinum monolith catalyst. *Appl. Catal. B Environ.* **2007**, *70*, 305–313.
69. Roh, H.S.; Lee, D.K.; Koo, K.Y.; Jung, U.H.; Yoon, W.L. Natural gas steam reforming for hydrogen production over metal monolith catalyst with efficient heat-transfer. *Int. J. Hydrogen Energy* **2010**, *35*, 1613–1619. [CrossRef]
70. Liu, W.; Hu, J.; Wang, Y. Fischer-Tropsch synthesis on ceramic monolith-structured catalysts. *Catal. Today* **2009**, *140*, 142–148. [CrossRef]
71. Boger, T.; Roy, S.; Heibel, A.K.; Borchers, O. A monolith loop reactor as an attractive alternative to slurry reactors. *Catal. Today* **2003**, *79–80*, 441–451. [CrossRef]
72. Yuan, H.; Sun, Z.; Liu, H.; Zhang, B.; Chen, C.; Wang, H.; Yang, Z.; Zhang, J.; Wei, F.; Su, D.S. Immobilizing Carbon Nanotubes on SiC Foam as a Monolith Catalyst for Oxidative Dehydrogenation Reactions. *ChemCatChem* **2013**, *5*, 1713–1717.
73. Duong-Viet, C.; Ba, H.; El-Berrichi, Z.; Nhut, J.M.; Ledoux, M.J.; Liu, Y.; Pham-Huu, C. Silicon carbide foam as a porous support platform for catalytic applications. *New J. Chem.* **2016**, *40*, 4285–4299. [CrossRef]
74. Sang, L.; Sun, B.; Tan, H.; Du, C.; Wu, Y.; Ma, C. Catalytic reforming of methane with CO_2 over metal foam based monolithic catalysts. *Int. J. Hydrogen Energy* **2012**, *37*, 13037–13043. [CrossRef]
75. Tariq, F.; Lee, P.D.; Haswell, R.; McComb, D.W. The influence of nanoscale microstructural variations on the pellet scale flow properties of hierarchical porous catalytic structures using multiscale 3D imaging. *Chem. Eng. Sci.* **2011**, *66*, 5804–5812. [CrossRef]
76. Wakao, N.; Smith, J.M. Diffusion in catalyst pellets. *Chem. Eng. Sci.* **1962**, *17*, 825–834. [CrossRef]
77. Saien, J.; Asgari, M.; Soleymani, A.R.; Taghavinia, N. Photocatalytic decomposition of direct red 16 and kinetics analysis in a conic body packed bed reactor with nanostructure titania coated Raschig rings. *Chem. Eng. J.* **2009**, *151*, 295–301. [CrossRef]
78. Tofighy, M.A.; Shirazi, Y.; Mohammadi, T.; Pak, A. Salty water desalination using carbon nanotubes membrane. *Chem. Eng. J.* **2011**, *168*, 1064–1072. [CrossRef]
79. Ziaka, Z.D.; Minet, R.G.; Tsotsis, T.T. A high temperature catalytic membrane reactor for propane dehydrogenation. *J. Memb. Sci.* **1993**, *77*, 221–232. [CrossRef]
80. Weyten, H.; Luyten, J.; Keizer, K.; Willems, L.; Leysen, R. Membrane performance: The key issues for dehydrogenation reactions in a catalytic membrane reactor. *Catal. Today* **2000**, *56*, 3–11. [CrossRef]
81. Champagnie, A.M.; Tsotsis, T.T.; Minet, R.G.; Webster, A.I. A high temperature catalytic membrane reactor for ethane dehydrogenation. *Chem. Eng. Sci.* **1990**, *45*, 2423–2429. [CrossRef]
82. Yarova, S.; Jones, D.; Jaouen, F.; Cavaliere, S. Strategies to Hierarchical Porosity in Carbon Nanofiber Webs for Electrochemical Applications. *Surfaces* **2019**, *2*, 13. [CrossRef]
83. Qin, Y.H.; Yang, H.H.; Zhang, X.S.; Li, P.; Zhou, X.G.; Niu, L.; Yuan, W.K. Electrophoretic deposition of network-like carbon nanofibers as a palladium catalyst support for ethanol oxidation in alkaline media. *Carbon* **2010**, *48*, 3323–3329. [CrossRef]
84. Sherigara, B.S.; Kutner, W.; D'Souza, F. Electrocatalytic Properties and Sensor Applications of Fullerenes and Carbon Nanotubes. *Electroanalysis* **2003**, *15*, 753–772. [CrossRef]
85. Daristotle, J.L.; Behrens, A.M.; Sandler, A.D.; Kofinas, P. A Review of the Fundamental Principles and Applications of Solution Blow Spinning. *ACS Appl. Mater. Interfaces* **2016**, *8*, 34951–34963. [CrossRef]
86. Li, D.; Xia, Y. Electrospinning of Nanofibers: Reinventing the Wheel? *Adv. Mater.* **2004**, *16*, 1151–1170. [CrossRef]
87. Xiao, Y.; Xu, Y.; Zhang, K.; Tang, X.; Huang, J.; Yuan, K.; Chen, Y. Coaxial electrospun free-standing and mechanical stable hierarchical porous carbon nanofiber membrane for flexible supercapacitors. *Carbon* **2020**, *160*, 80–87. [CrossRef]
88. Li, B.; Ge, X.; Goh, F.W.T.; Hor, T.S.A.; Geng, D.; Du, G.; Liu, Z.; Zhang, J.; Liu, X.; Zong, Y. Co_3O_4 nanoparticles decorated carbon nanofiber mat as binder-free air-cathode for high performance rechargeable zinc-air batteries. *Nanoscale* **2015**, *7*, 1830–1838. [CrossRef]

89. De Poulpiquet, A.; Marques-Knopf, H.; Wernert, V.; Giudici-Orticoni, M.T.; Gadiou, R.; Lojou, E. Carbon nanofiber mesoporous films: Efficient platforms for bio-hydrogen oxidation in biofuel cells. *Phys. Chem. Chem. Phys.* **2014**, *16*, 1366–1378. [CrossRef]
90. Kumar, B.; Asadi, M.; Pisasale, D.; Sinha-Ray, S.; Rosen, B.A.; Haasch, R.; Abiade, J.; Yarin, A.L.; Salehi-Khojin, A. Renewable and metal-free carbon nanofibre catalysts for carbon dioxide reduction. *Nat. Commun.* **2013**, *4*, 2819. [CrossRef]
91. Wangxi, Z.; Jie, L.; Gang, W. Evolution of structure and properties of PAN precursors during their conversion to carbon fibers. *Carbon* **2003**, *41*, 2805–2812. [CrossRef]
92. Mittal, J.; Mathur, R.B.; Bahl, O.P. Post spinning modification of pan fibres—A review. *Carbon* **1997**, *35*, 1713–1721. [CrossRef]
93. Han, Y.; Li, R.; Brückner, C.; Vadas, T. Controlling the Surface Oxygen Groups of Polyacrylonitrile-Based Carbon Nanofiber Membranes While Limiting Fiber Degradation. *C J. Carbon Res.* **2018**, *4*, 40. [CrossRef]
94. Bai, Y.; Huang, Z.H.; Kang, F. Surface oxidation of activated electrospun carbon nanofibers and their adsorption performance for benzene, butanone and ethanol. *Colloids Surf. A Physicochem. Eng. Asp.* **2014**, *443*, 66–71. [CrossRef]
95. Wang, M.X.; Huang, Z.H.; Shimohara, T.; Kang, F.; Liang, K. NO removal by electrospun porous carbon nanofibers at room temperature. *Chem. Eng. J.* **2011**, *170*, 505–511. [CrossRef]
96. Zhang, L.; Fan, W.; Liu, T. Flexible hierarchical membranes of WS2 nanosheets grown on graphene-wrapped electrospun carbon nanofibers as advanced anodes for highly reversible lithium storage. *Nanoscale* **2016**, *8*, 16387–16394. [CrossRef]
97. Zhong, Y.; Qiu, X.; Chen, D.; Li, N.; Xu, Q.; Li, H.; He, J.; Lu, J. Flexible Electrospun Carbon Nanofiber/Tin(IV) Sulfide Core/Sheath Membranes for Photocatalytically Treating Chromium(VI)-Containing Wastewater. *ACS Appl. Mater. Interfaces* **2016**, *8*, 28671–28677. [CrossRef] [PubMed]
98. Faccini, M.; Borja, G.; Boerrigter, M.; Martín, D.M.; Crespiera, S.M.; Vázquez-Campos, S.; Aubouy, L.; Amantia, D. Electrospun Carbon Nanofiber Membranes for Filtration of Nanoparticles from Water. *J. Nanomater.* **2015**, *2015*, 247471. [CrossRef]
99. Tian, J.; Shi, Y.; Fan, W.; Liu, T. Ditungsten carbide nanoparticles embedded in electrospun carbon nanofiber membranes as flexible and high-performance supercapacitor electrodes. *Compos. Commun.* **2019**, *12*, 21–25. [CrossRef]
100. Liu, D.; Zhang, X.; Sun, Z.; You, T. Free-standing nitrogen-doped carbon nanofiber films as highly efficient electrocatalysts for oxygen reduction. *Nanoscale* **2013**, *5*, 9528–9531. [CrossRef] [PubMed]
101. Ji, D.; Peng, S.; Lu, J.; Li, L.; Yang, S.; Yang, G.; Qin, X.; Srinivasan, M.; Ramakrishna, S. Design and synthesis of porous channel-rich carbon nanofibers for self-standing oxygen reduction reaction and hydrogen evolution reaction bifunctional catalysts in alkaline medium. *J. Mater. Chem. A* **2017**, *5*, 7507–7515. [CrossRef]
102. Wang, C.; Kim, J.; Kim, M.; Lim, H.; Zhang, M.; You, J.; Yun, J.H.; Bando, Y.; Li, J.; Yamauchi, Y. Nanoarchitectured metal-organic framework-derived hollow carbon nanofiber filters for advanced oxidation processes. *J. Mater. Chem. A* **2019**, *7*, 13743–13750. [CrossRef]
103. Miao, Y.E.; Li, F.; Lu, H.; Yan, J.; Huang, Y.; Liu, T. Nanocubic-Co_3O_4 coupled with nitrogen-doped carbon nanofiber network: A synergistic binder-free catalyst toward oxygen reduction reactions. *Compos. Commun.* **2016**, *1*, 15–19. [CrossRef]
104. Yan, J.; Lu, H.; Huang, Y.; Fu, J.; Mo, S.; Wei, C.; Miao, Y.E.; Liu, T. Polydopamine-derived porous carbon fiber/cobalt composites for efficient oxygen reduction reactions. *J. Mater. Chem. A* **2015**, *3*, 23299–23306. [CrossRef]
105. Liu, Y.; Jiang, G.; Sun, S.; Xu, B.; Zhou, J.; Zhang, Y.; Yao, J. Growth of NiCo2S4 nanotubes on carbon nanofibers for high performance flexible supercapacitors. *J. Electroanal. Chem.* **2017**, *804*, 212–219. [CrossRef]
106. Zhao, F.; Zhao, X.; Peng, B.; Gan, F.; Yao, M.; Tan, W.; Dong, J.; Zhang, Q. Polyimide-derived carbon nanofiber membranes as anodes for high-performance flexible lithium ion batteries. *Chin. Chem. Lett.* **2018**, *29*, 1692–1697. [CrossRef]
107. Bai, Y.; Huang, Z.H.; Yu, X.; Kaneko, K.; Kang, F. Micro-mesoporous graphitic carbon nanofiber membranes. *Carbon* **2018**, *132*, 746–748. [CrossRef]
108. Liu, M.; Du, Y.; Miao, Y.E.; Ding, Q.; He, S.; Tjiu, W.W.; Pan, J.; Liu, T. Anisotropic conductive films based on highly aligned polyimide fibers containing hybrid materials of graphene nanoribbons and carbon nanotubes. *Nanoscale* **2015**, *7*, 1037–1046. [PubMed]

109. Longtin, R.; Fauteux, C.; Goduguchinta, R.; Pegna, J. Synthesis of carbon nanofiber films and nanofiber composite coatings by laser-assisted catalytic chemical vapor deposition. *Thin Solid Films* **2007**, *515*, 2958–2964. [CrossRef]
110. Espinosa, R.B.; Rafieian, D.; Lammertink, R.G.H.; Lefferts, L. Carbon nano-fiber based membrane reactor for selective nitrite hydrogenation. *Catal. Today* **2016**, *273*, 50–61. [CrossRef]
111. García-Bordejé, E.; Kapteijn, F.; Moulijn, J.A. Preparation and characterisation of carbon-coated monoliths for catalyst supports. *Carbon* **2002**, *40*, 1079–1088.
112. Tu, J.P.; Zhu, L.P.; Hou, K.; Guo, S.Y. Synthesis and frictional properties of array film of amorphous carbon nanofibers on anodic aluminum oxide. *Carbon* **2003**, *41*, 1257–1263.
113. Huang, S.; Dai, L.; Mau, A.W.H. Controlled Fabrication of Large-Scale Aligned Carbon Nanofiber/Nanotube Patterns by Photolithography. *Adv. Mater.* **2002**, *14*, 1140–1143.
114. Melechko, A.V.; McKnight, T.E.; Hensley, D.K.; Guillorn, M.A.; Borisevich, A.Y.; Merkulov, V.I.; Lowndes, D.H.; Simpson, M.L. Large-scale synthesis of arrays of high-aspect-ratio rigid vertically aligned carbon nanofibres. *Nanotechnology* **2003**, *14*, 1029–1035.
115. Elangovan, A.; Xu, J.; Brown, E.; Liu, B.; Li, J. Fundamental Electrochemical Insights of Vertically Aligned Carbon Nanofiber Architecture as a Catalyst Support for ORR. *J. Electrochem. Soc.* **2020**, *167*, 066523.
116. Arumugam, P.U.; Chen, H.; Siddiqui, S.; Weinrich, J.A.P.; Jejelowo, A.; Li, J.; Meyyappan, M. Wafer-scale fabrication of patterned carbon nanofiber nanoelectrode arrays: A route for development of multiplexed, ultrasensitive disposable biosensors. *Biosens. Bioelectron.* **2009**, *24*, 2818–2824. [PubMed]
117. Thakur, D.B.; Tiggelaar, R.M.; Weber, Y.; Gardeniers, J.G.E.; Lefferts, L.; Seshan, K. Ruthenium catalyst on carbon nanofiber support layers for use in silicon-based structured microreactors. Part II: Catalytic reduction of bromate contaminants in aqueous phase. *Appl. Catal. B Environ.* **2011**, *102*, 243–250. [CrossRef]
118. Laurila, T.; Sainio, S.; Jiang, H.; Isoaho, N.; Koehne, J.E.; Etula, J.; Koskinen, J.; Meyyappan, M. Application-Specific Catalyst Layers: Pt-Containing Carbon Nanofibers for Hydrogen Peroxide Detection. *ACS Omega* **2017**, *2*, 496–507. [CrossRef] [PubMed]
119. Shawat, E.; Perelshtein, I.; Westover, A.; Pint, C.L.; Nessim, G.D. Ultra high-yield one-step synthesis of conductive and superhydrophobic three-dimensional mats of carbon nanofibers via full catalysis of unconstrained thin films. *J. Mater. Chem. A* **2014**, *2*, 15118–15123. [CrossRef]
120. Park, K.H.; Yim, J.H.; Lee, S.; Koh, K.H. Catalyst-assisted hot filament chemical vapor deposition and characterization of carbon nanostructures. In *Thin Solid Films*; Elsevier: Amsterdam, The Netherlands, 2006; pp. 233–237.
121. Nerushev, O.A.; Sveningsson, M.; Falk, L.K.L.; Rohmund, F. Carbon nanotube films obtained by thermal chemical vapour deposition. *J. Mater. Chem.* **2001**, *11*, 1122–1132. [CrossRef]
122. Singh, C.; Shaffer, M.S.P.; Windle, A.H. Production of controlled architectures of aligned carbon nanotubes by an injection chemical vapour deposition method. *Carbon* **2003**, *41*, 359–368. [CrossRef]
123. Kamada, K.; Ikuno, T.; Takahashi, S.; Oyama, T.; Yamamoto, T.; Kamizono, M.; Ohkura, S.; Honda, S.; Katayama, M.; Hirao, T.; et al. Surface morphology and field emission characteristics of carbon nanofiber films grown by chemical vapor deposition on alloy catalyst. *Appl. Surf. Sci* **2003**, *212*, 383–387. [CrossRef]
124. Shah, K.A.; Tali, B.A. Synthesis of carbon nanotubes by catalytic chemical vapour deposition: A review on carbon sources, catalysts and substrates. *Mater. Sci. Semicond. Process.* **2016**, *41*, 67–82. [CrossRef]
125. Hashim, D.P.; Narayanan, N.T.; Romo-Herrera, J.M.; Cullen, D.A.; Hahm, M.G.; Lezzi, P.; Suttle, J.R.; Kelkhoff, D.; Muñoz-Sandoval, E.; Ganguli, S.; et al. Covalently bonded three-dimensional carbon nanotube solids via boron induced nanojunctions. *Sci. Rep.* **2012**, *2*, 363. [CrossRef]
126. Kaskela, A.; Nasibulin, A.G.; Timmermans, M.Y.; Aitchison, B.; Papadimitratos, A.; Tian, Y.; Zhu, Z.; Jiang, H.; Brown, D.P.; Zakhidov, A.; et al. Aerosol-synthesized SWCNT networks with tunable conductivity and transparency by a dry transfer technique. *Nano Lett.* **2010**, *10*, 4349–4355. [CrossRef]
127. Zhilyaeva, M.A.; Shulga, E.V.; Shandakov, S.D.; Sergeichev, I.V.; Gilshteyn, E.P.; Anisimov, A.S.; Nasibulin, A.G. A novel straightforward wet pulling technique to fabricate carbon nanotube fibers. *Carbon* **2019**, *150*, 69–75. [CrossRef]
128. Werder, T.; Walther, J.H.; Jaffe, R.L.; Halicioglu, T.; Noca, F.; Koumoutsakos, P. Molecular Dynamics Simulation of Contact Angles of Water Droplets in Carbon Nanotubes. *Nano Lett.* **2001**, *1*, 697–702. [CrossRef]
129. Ma, P.-C.; Siddiqui, N.A.; Marom, G.; Kim, J.-K. Dispersion and functionalization of carbon nanotubes for polymer-based nanocomposites: A review. *Compos. Part A Appl. Sci. Manuf.* **2010**, *41*, 1345–1367. [CrossRef]

130. Clark, M.D.; Subramanian, S.; Krishnamoorti, R. Understanding surfactant aided aqueous dispersion of multi-walled carbon nanotubes. *J. Colloid Interface Sci.* **2011**, *354*, 144–151. [CrossRef] [PubMed]
131. Wu, Z.; Chen, Z.; Du, X.; Logan, J.M.; Sippel, J.; Nikolou, M.; Kamaras, K.; Reynolds, J.R.; Tanner, D.B.; Hebard, A.F.; et al. Transparent, conductive carbon nanotube films. *Science* **2004**, *305*, 1273–1276. [CrossRef]
132. Liang, L.; Gao, C.; Chen, G.; Guo, C.Y. Large-area, stretchable, super flexible and mechanically stable thermoelectric films of polymer/carbon nanotube composites. *J. Mater. Chem. C* **2016**, *4*, 526–532. [CrossRef]
133. He, X.; Gao, W.; Xie, L.; Li, B.; Zhang, Q.; Lei, S.; Robinson, J.M.; Hroz, E.H.; Doorn, S.K.; Wang, W.; et al. Wafer-scale monodomain films of spontaneously aligned single-walled carbon nanotubes. *Nat. Nanotechnol.* **2016**, *11*, 633–638. [CrossRef]
134. Lee, K.; Lee, S.S.; Lee, J.A.; Lee, K.C.; Ji, S. Carbon nanotube film piezoresistors embedded in polymer membranes. *Appl. Phys. Lett.* **2010**, *96*, 013511. [CrossRef]
135. Jia, Y.; Li, P.; Wei, J.; Cao, A.; Wang, K.; Li, C.; Zhuang, D.; Zhu, H.; Wu, D. Carbon nanotube films by filtration for nanotube-silicon heterojunction solar cells. *Mater. Res. Bull.* **2010**, *45*, 1401–1405. [CrossRef]
136. Chew, S.Y.; Ng, S.H.; Wang, J.; Novák, P.; Krumeich, F.; Chou, S.L.; Chen, J.; Liu, H.K. Flexible free-standing carbon nanotube films for model lithium-ion batteries. *Carbon* **2009**, *47*, 2976–2983. [CrossRef]
137. Woo, C.S.; Lim, C.H.; Cho, C.W.; Park, B.; Ju, H.; Min, D.H.; Lee, C.J.; Lee, S.B. Fabrication of flexible and transparent single-wall carbon nanotube gas sensors by vacuum filtration and poly(dimethyl siloxane) mold transfer. *Microelectron. Eng.* **2007**, *84*, 1610–1613. [CrossRef]
138. Zhou, Y.; Hu, L.; Grüner, G. A method of printing carbon nanotube thin films. *Appl. Phys. Lett.* **2006**, *88*, 123109. [CrossRef]
139. Rojas, J.A.; Ardila-Rodríguez, L.A.; Diniz, M.F.; Gonçalves, M.; Ribeiro, B.; Rezende, M.C. Optimization of Triton X-100 removal and ultrasound probe parameters in the preparation of multiwalled carbon nanotube buckypaper. *Mater. Des.* **2019**, *166*, 107612. [CrossRef]
140. Restivo, J.; Orge, C.A.; Santos, A.S.G.G.; Soares, O.S.G.P.; Pereira, M.F.R. Nanostructured Layers of Mechanically Processed Multiwalled Carbon Nanotubes for Catalytic Ozonation of Organic Pollutants. *ACS Appl. Nano Mater.* **2020**, *3*, 5271–5284. [CrossRef]
141. Geng, Y.; Liu, M.Y.; Li, J.; Shi, X.M.; Kim, J.K. Effects of surfactant treatment on mechanical and electrical properties of CNT/epoxy nanocomposites. *Compos. Part A Appl. Sci. Manuf.* **2008**, *39*, 1876–1883. [CrossRef]
142. Tchoul, M.N.; Ford, W.T.; Lolli, G.; Resasco, D.E.; Arepalli, S. Effect of Mild Nitric Acid Oxidation on Dispersability, Size, and Structure of Single-Walled Carbon Nanotubes. *Chem. Mater.* **2007**, *19*, 5765–5772. [CrossRef]
143. Faria, P.C.C.; Órfão, J.J.M.; Pereira, M.F.R. Adsorption of anionic and cationic dyes on activated carbons with different surface chemistries. *Water Res.* **2004**, *38*, 2043–2052. [CrossRef]
144. Liu, Z.Q.; Ma, J.; Cui, Y.H.; Zhang, B.P. Effect of ozonation pretreatment on the surface properties and catalytic activity of multi-walled carbon nanotube. *Appl. Catal. B Environ.* **2009**, *92*, 301–306. [CrossRef]
145. Sousa, J.P.S.; Pereira, M.F.R.; Figueiredo, J.L. Catalytic oxidation of NO to NO_2 on N-doped activated carbons. *Catal. Today* **2011**, *176*, 383–387. [CrossRef]
146. Figueiredo, J.L.; Pereira, M.F.R. The role of surface chemistry in catalysis with carbons. *Catal. Today* **2010**, *150*, 2–7. [CrossRef]
147. Hill, D.E.; Lin, Y.; Rao, A.M.; Allard, L.F.; Sun, Y.P. Functionalization of carbon nanotubes with polystyrene. *Macromolecules* **2002**, *35*, 9466–9471. [CrossRef]
148. Shen, J.N.; Yu, C.C.; Ruan, H.M.; Gao, C.J.; Van der Bruggen, B. Preparation and characterization of thin-film nanocomposite membranes embedded with poly(methyl methacrylate) hydrophobic modified multiwalled carbon nanotubes by interfacial polymerization. *J. Memb. Sci.* **2013**, *442*, 18–26. [CrossRef]
149. Patel, S.C.; Alam, O.; Zhang, D.; Grover, K.; Qin, Y.X.; Sitharaman, B. Layer-by-layer, ultrasonic spray assembled 2D and 3D chemically crosslinked carbon nanotubes and graphene. *J. Mater. Res.* **2017**, *32*, 370–382. [CrossRef]
150. Katz, E.; Willner, I. Biomolecule-functionalized carbon nanotubes: Applications in nanobioelectronics. *ChemPhysChem* **2004**, *5*, 1084–1104. [CrossRef]
151. Darsono, N.; Yoon, D.-H.; Kim, J. Milling and dispersion of multi-walled carbon nanotubes in texanol. *Appl. Surf. Sci.* **2008**, *254*, 3412–3419. [CrossRef]
152. Munkhbayar, B.; Nine, M.J.; Jeoun, J.; Bat-Erdene, M.; Chung, H.; Jeong, H. Influence of dry and wet ball milling on dispersion characteristics of the multi-walled carbon nanotubes in aqueous solution with and without surfactant. *Powder Technol.* **2013**, *234*, 132–140. [CrossRef]

153. Lee, J.H.; Kong, B.S.; Yang, S.B.; Jung, H.T. Fabrication of single-walled carbon nanotube/tin nanoparticle composites by electrochemical reduction combined with vacuum filtration and hybrid co-filtration for high-performance lithium battery electrodes. *J. Power Sources* **2009**, *194*, 520–525. [CrossRef]
154. Ansón-Casaos, A.; González-Domínguez, J.M.; Terrado, E.; Martínez, M.T. Surfactant-free assembling of functionalized single-walled carbon nanotube buckypapers. *Carbon* **2010**, *48*, 1480–1488. [CrossRef]
155. Ham, H.T.; Choi, Y.S.; Chung, I.J. An explanation of dispersion states of single-walled carbon nanotubes in solvents and aqueous surfactant solutions using solubility parameters. *J. Colloid Interface Sci.* **2005**, *286*, 216–223. [CrossRef]
156. Sun, J.; Gao, L.; Li, W. Colloidal Processing of Carbon Nanotube/Alumina Composites. *Chem. Mater.* **2002**, *14*, 5169–5172. [CrossRef]
157. Le, H.R.; Howson, A.; Ramanauskas, M.; Williams, J.A. Tribological Characterisation of Air-Sprayed Epoxy-CNT Nanocomposite Coatings. *Tribol. Lett.* **2011**, *45*, 301–308. [CrossRef]
158. Ozden, S.; Tsafack, T.; Owuor, P.S.; Li, Y.; Jalilov, A.S.; Vajtai, R.; Tiwary, C.S.; Lou, J.; Tour, J.M.; Mohite, A.D.; et al. Chemically interconnected light-weight 3D-carbon nanotube solid network. *Carbon* **2017**, *119*, 142–149. [CrossRef]
159. Lalwani, G.; Kwaczala, A.T.; Kanakia, S.; Patel, S.C.; Judex, S.; Sitharaman, B. Fabrication and characterization of three-dimensional macroscopic all-carbon scaffolds. *Carbon* **2013**, *53*, 90–100. [CrossRef] [PubMed]
160. Ozden, S.; Narayanan, T.N.; Tiwary, C.S.; Dong, P.; Hart, A.H.C.; Vajtai, R.; Ajayan, P.M. 3D Macroporous Solids from Chemically Cross-linked Carbon Nanotubes. *Small* **2015**, *11*, 688–693. [CrossRef]
161. Kim, K.H.; Oh, Y.; Islam, M.F. Graphene coating makes carbon nanotube aerogels superelastic and resistant to fatigue. *Nat. Nanotechnol.* **2012**, *7*, 562–566. [CrossRef] [PubMed]
162. Dumée, L.; Germain, V.; Sears, K.; Schütz, J.; Finn, N.; Duke, M.; Cerneaux, S.; Cornu, D.; Gray, S. Enhanced durability and hydrophobicity of carbon nanotube bucky paper membranes in membrane distillation. *J. Memb. Sci.* **2011**, *376*, 241–246. [CrossRef]
163. Zhu, Y.; Yu, L.; Wang, X.; Zhou, Y.; Ye, H. A novel monolithic Pd catalyst supported on cordierite with graphene coating. *Catal. Commun.* **2013**, *40*, 98–102. [CrossRef]
164. Zhu, Y.; Zhou, Y.; Yu, L.; Liu, G.; Tian, Y.; Ye, H. A highly stable and active Pd catalyst on monolithic cordierite with graphene coating assisted by PDDA. *RSC Adv.* **2014**, *4*, 9480–9483. [CrossRef]
165. Sarkar, A.; Daniels-Race, T. Electrophoretic Deposition of Carbon Nanotubes on 3-Amino-Propyl-Triethoxysilane (APTES) Surface Functionalized Silicon Substrates. *Nanomaterials* **2013**, *3*, 272–288. [CrossRef]
166. Mansfield, E.; Feldman, A.; Chiaramonti, A.N.; Lehman, J.; Curtin, A.E. Morphological and electrical characterization of MWCNT papers and pellets. *J. Res. Natl. Inst. Stand. Technol.* **2015**, *120*, 304–315. [CrossRef]
167. Yi, C.W.; Luo, K.; Wei, T.; Goodman, D.W. The composition and structure of Pd–Au surfaces. *J. Phys. Chem. B* **2005**, *109*, 18535–18540. [CrossRef]
168. Urper, O.; Çakmak, İ.; Karatepe, N. Fabrication of carbon nanotube transparent conductive films by vacuum filtration method. *Mater. Lett.* **2018**, *223*, 210–214. [CrossRef]
169. Tambasov, I.A.; Voronin, A.S.; Evsevskaya, N.P.; Volochaev, M.N.; Fadeev, Y.V.; Simunin, M.M.; Aleksandrovsky, A.S.; Smolyarova, T.; Abelian, S.R.; Tambasova, E.V.; et al. Thermoelectric properties of low-cost transparent single wall carbon nanotube thin films obtained by vacuum filtration. *Phys. E Low-Dimens. Syst. Nanostruct.* **2019**, *114*, 113619. [CrossRef]
170. Qian, M.; Feng, T.; Wang, K.; Ding, H.; Chen, Y.; Sun, Z. A comparative study of field emission properties of carbon nanotube films prepared by vacuum filtration and screen-printing. *Appl. Surf. Sci.* **2010**, *256*, 4642–4646. [CrossRef]
171. Goh, K.; Jiang, W.; Karahan, H.E.; Zhai, S.; Wei, L.; Yu, D.; Fane, A.G.; Wang, R.; Chen, Y. All-carbon nanoarchitectures as high-performance separation membranes with superior stability. *Adv. Funct. Mater.* **2015**, *25*, 7348–7359. [CrossRef]
172. Yang, H.Y.; Han, Z.J.; Yu, S.F.; Pey, K.L.; Ostrikov, K.; Karnik, R. Carbon nanotube membranes with ultrahigh specific adsorption capacity for water desalination and purification. *Nat. Commun.* **2013**, *4*, 2220. [CrossRef] [PubMed]
173. Ostojic, G.N.; Liang, Y.T.; Hersam, M.C. Catalytically active nanocomposites of electronically coupled carbon nanotubes and platinum nanoparticles formed via vacuum filtration. *Nanotechnology* **2009**, *20*, 434019. [CrossRef]

174. Zhang, L.; Gu, J.; Song, L.; Chen, L.; Huang, Y.; Zhang, J.; Chen, T. Underwater superoleophobic carbon nanotubes/core-shell polystyrene@Au nanoparticles composite membrane for flow-through catalytic decomposition and oil/water separation. *J. Mater. Chem. A* **2016**, *4*, 10810–10815. [CrossRef]
175. Rao, P.S.; Wey, M.Y.; Tseng, H.H.; Kumar, I.A.; Weng, T.H. A comparison of carbon/nanotube molecular sieve membranes with polymer blend carbon molecular sieve membranes for the gas permeation application. *Microporous Mesoporous Mater.* **2008**, *113*, 499–510. [CrossRef]
176. Lalia, B.S.; Ahmed, F.E.; Shah, T.; Hilal, N.; Hashaikeh, R. Electrically conductive membranes based on carbon nanostructures for self-cleaning of biofouling. *Desalination* **2015**, *360*, 8–12. [CrossRef]
177. Omi, F.R.; Choudhury, M.R.; Anwar, N.; Bakr, A.R.; Rahaman, M.S. Highly Conductive Ultrafiltration Membrane via Vacuum Filtration Assisted Layer-by-Layer Deposition of Functionalized Carbon Nanotubes. *Ind. Eng. Chem. Res.* **2017**, *56*, 8474–8484. [CrossRef]
178. Wang, Y.; Zhang, L.; Wang, P. Self-Floating Carbon Nanotube Membrane on Macroporous Silica Substrate for Highly Efficient Solar-Driven Interfacial Water Evaporation. *ACS Sustain. Chem. Eng.* **2016**, *4*, 1223–1230. [CrossRef]
179. Chan, W.F.; Chen, H.Y.; Surapathi, A.; Taylor, M.G.; Shao, X.; Marand, E.; Johnson, J.K. Zwitterion functionalized carbon nanotube/polyamide nanocomposite membranes for water desalination. *ACS Nano* **2013**, *7*, 5308–5319. [CrossRef]
180. Lee, H.D.; Kim, H.W.; Cho, Y.H.; Park, H.B. Experimental Evidence of Rapid Water Transport through Carbon Nanotubes Embedded in Polymeric Desalination Membranes. *Small* **2014**, *10*, 2653–2660. [CrossRef]
181. Wu, L.; Zhang, X.; Ju, H. Detection of NADH and Ethanol Based on Catalytic Activity of Soluble Carbon Nanofiber with Low Overpotential. *Anal. Chem.* **2007**, *79*, 453–458. [CrossRef] [PubMed]
182. Maiyalagan, T. Silicotungstic acid stabilized Pt-Ru nanoparticles supported on carbon nanofibers electrodes for methanol oxidation. *Int. J. Hydrogen Energy* **2009**, *34*, 2874–2879. [CrossRef]
183. Gan, L.; Du, H.; Li, B.; Kang, F. Enhanced oxygen reduction performance of Pt catalysts by nano-loops formed on the surface of carbon nanofiber support. *Carbon* **2008**, *46*, 2140–2143. [CrossRef]
184. Zhang, G.Q.; Zheng, J.P.; Liang, R.; Zhang, C.; Wang, B.; Au, M.; Hendrickson, M.; Plichta, E.J. α-MnO_2/Carbon Nanotube/Carbon Nanofiber Composite Catalytic Air Electrodes for Rechargeable Lithium-air Batteries. *J. Electrochem. Soc.* **2011**, *158*, A822. [CrossRef]
185. Baig, N.; Alghunaimi, F.I.; Dossary, H.S.; Saleh, T.A. Superhydrophobic and superoleophilic carbon nanofiber grafted polyurethane for oil-water separation. *Process Saf. Environ. Prot.* **2019**, *123*, 327–334. [CrossRef]
186. Kiadehi, A.D.; Jahanshahi, M.; Rahimpour, A.; Ghoreyshi, S.A.A. The effect of functionalized carbon nano-fiber (CNF) on gas separation performance of polysulfone (PSf) membranes. *Chem. Eng. Process. Process Intensif.* **2015**, *90*, 41–48. [CrossRef]
187. Zainoodin, A.M.; Kamarudin, S.K.; Masdar, M.S.; Daud, W.R.W.; Mohamad, A.B.; Sahari, J. High power direct methanol fuel cell with a porous carbon nanofiber anode layer. *Appl. Energy* **2014**, *113*, 946–954. [CrossRef]
188. Simescu-Lazar, F.; Chaieb, T.; Pallier, S.; Veyre, L.; Philippe, R.; Meille, V. Direct coating of carbon-supported catalysts on monoliths and foams—Singular behaviour of Pd/MWCNT. *Appl. Catal. A Gen.* **2015**, *508*, 45–51. [CrossRef]
189. Rodriguez, P.; Simescu-Lazar, F.; Meille, V.; Bah, T.; Pallier, S.; Fournel, I. Carbon-coated structured supports. Preparation and use for nitrobenzene hydrogenation. *Appl. Catal. A Gen.* **2012**, *427–428*, 66–72. [CrossRef]
190. Liu, Y.; Ba, H.; Nguyen, D.-L.; Ersen, O.; Romero, T.; Zafeiratos, S.; Begin, D.; Janowska, I.; Pham-Huu, C. Synthesis of porous carbon nanotubes foam composites with a high accessible surface area and tunable porosity. *J. Mater. Chem. A* **2013**, *1*, 9508–9516. [CrossRef]
191. Mirri, F.; Ma, A.W.K.; Hsu, T.T.; Behabtu, N.; Eichmann, S.L.; Young, C.C.; Tsentalovich, D.E.; Pasquali, M. High-performance carbon nanotube transparent conductive films by scalable dip coating. *ACS Nano* **2012**, *6*, 9737–9744. [CrossRef] [PubMed]
192. Thomas, B.J.C.; Boccaccini, A.R.; Shaffer, M.S.P. Multi-Walled Carbon Nanotube Coatings Using Electrophoretic Deposition (EPD). *J. Am. Ceram. Soc.* **2005**, *88*, 980–982. [CrossRef]
193. Liu, C.; Long, Y.; Magdassi, S.; Mandler, D. Ionic strength induced electrodeposition: A universal approach for nanomaterial deposition at selective areas. *Nanoscale* **2017**, *9*, 485–490. [CrossRef] [PubMed]
194. Tahar, A.B.; Romdhane, A.; Lalaoui, N.; Reverdy-Bruas, N.; le Goff, A.; Holzinger, M.; Cosnier, S.; Chaussy, D.; Belgacem, N. Carbon nanotube-based flexible biocathode for enzymatic biofuel cells by spray coating. *J. Power Sources* **2018**, *408*, 1–6. [CrossRef]

195. Hossain, M.A.; Wang, M.; Choy, K.L. Ecofriendly and Nonvacuum Electrostatic Spray-Assisted Vapor Deposition of Cu(In,Ga)(S,Se)$_2$ Thin Film Solar Cells. *ACS Appl. Mater. Interfaces* **2015**, *7*, 22497–22503. [CrossRef]
196. Bondavalli, P.; Delfaure, C.; Legagneux, P.; Pribat, D. Supercapacitor Electrode Based on Mixtures of Graphite and Carbon Nanotubes Deposited Using a Dynamic Air-Brush Deposition Technique. *J. Electrochem. Soc.* **2013**, *160*, A601–A606. [CrossRef]
197. Kim, S.; Yim, J.; Wang, X.; Bradley, D.D.C.; Lee, S.; DeMello, J.C. Spin-and spray-deposited single-walled carbon-nanotube electrodes for organic solar cells. *Adv. Funct. Mater.* **2010**, *20*, 2310–2316. [CrossRef]
198. Palgrave, R.G.; Parkin, I.P. Aerosol Assisted Chemical Vapor Deposition Using Nanoparticle Precursors: A Route to Nanocomposite Thin Films. *J. Am. Chem. Soc.* **2006**, *128*, 1587–1597. [CrossRef] [PubMed]
199. Xiang, C.; Lu, W.; Zhu, Y.; Sun, Z.; Yan, Z.; Hwang, C.C.; Tour, J.M. Carbon nanotube and graphene nanoribbon-coated conductive Kevlar fibers. *ACS Appl. Mater. Interfaces* **2012**, *4*, 131–136. [CrossRef] [PubMed]
200. Choy, K.-L. *Innovative Processing of Films and Nanocrystalline Powders*; Imperial College Press: London, UK, 2002.
201. Muhlbauer, R.L.; Pruyn, T.L.; Puckett, W.T.; Gerhardt, R.A. Effect of graphitic filler size and shape on the microstructure, electrical percolation behavior and thermal properties of nanostructured multilayered carbon films deposited onto paper substrates. *J. Mater. Res.* **2014**, *29*, 472–484. [CrossRef]
202. David, L.; Asok, D.; Singh, G. Synthesis and extreme rate capability of Si-Al-C-N functionalized carbon nanotube spray-on coatings as li-ion battery electrode. *ACS Appl. Mater. Interfaces* **2014**, *6*, 16056–16064. [CrossRef] [PubMed]
203. Cho, S.; Takagi, K.; Kwon, H.; Seo, D.; Ogawa, K.; Kikuchi, K.; Kawasaki, A. Multi-walled carbon nanotube-reinforced copper nanocomposite coating fabricated by low-pressure cold spray process. *Surf. Coat. Technol.* **2012**, *206*, 3488–3494. [CrossRef]
204. Jo, J.W.; Jung, J.W.; Lee, J.U.; Jo, W.H. Fabrication of highly conductive and transparent thin films from single-walled carbon nanotubes using a new non-ionic surfactant via spin coating. *ACS Nano* **2010**, *4*, 5382–5388. [CrossRef] [PubMed]
205. Hellstrom, S.L.; Lee, H.W.; Bao, Z. Polymer-assisted direct deposition of uniform carbon nanotube bundle networks for high performance transparent electrodes. *ACS Nano* **2009**, *3*, 1423–1430. [CrossRef]
206. Yim, J.H.; Kim, Y.S.; Koh, K.H.; Lee, S. Fabrication of transparent single wall carbon nanotube films with low sheet resistance. *J. Vac. Sci. Technol. B Microelectron. Nanom. Struct.* **2008**, *26*, 851. [CrossRef]
207. Rakhi, R.B.; Sethupathi, K.; Ramaprabhu, S. Field emission from carbon nanotubes on a graphitized carbon fabric. *Carbon* **2008**, *46*, 1656–1663. [CrossRef]
208. Schmidt, R.H.; Kinloch, I.A.; Burgess, A.N.; Windle, A.H. The effect of aggregation on the electrical conductivity of spin-coated polymer/carbon nanotube composite films. *Langmuir* **2007**, *23*, 5707–5712. [CrossRef]
209. Di, Y.; Cui, Y.; Wang, Q.; Lei, W.; Zhang, X.; Den Engelsen, D. Field emission from carbon nanotube and tetrapod-like ZnO compound cathode fabricated by spin-coating method. *Appl. Surf. Sci.* **2009**, *255*, 4636–4639. [CrossRef]
210. Wei, B.Y.; Hsu, M.C.; Su, P.G.; Lin, H.M.; Wu, R.J.; Lai, H.J. A novel SnO_2 gas sensor doped with carbon nanotubes operating at room temperature. *Sens. Actuators B Chem.* **2004**, *101*, 81–89. [CrossRef]
211. He, L.; Jia, Y.; Meng, F.; Li, M.; Liu, J. Gas sensors for ammonia detection based on polyaniline-coated multi-wall carbon nanotubes. *Mater. Sci. Eng. B Solid State Mater. Adv. Technol.* **2009**, *163*, 76–81. [CrossRef]
212. Stéphan, C.; Nguyen, T.P.; De la Chapelle, M.L.; Lefrant, S.; Journet, C.; Bernier, P. Characterization of singlewalled carbon nanotubes-PMMA composites. *Synth. Met.* **2000**, *108*, 139–149. [CrossRef]
213. Fan, B.; Mei, X.; Sun, K.; Ouyang, J. Conducting polymer/carbon nanotube composite as counter electrode of dye-sensitized solar cells. *Appl. Phys. Lett.* **2008**, *93*, 143103. [CrossRef]
214. Yukui, L.; Changchun, Z.; Xinghui, L. Field emission display with carbon nanotubes cathode: Prepared by a screen-printing process. *Diam. Relat. Mater.* **2002**, *11*, 1845–1847. [CrossRef]
215. Shi, Y.S.; Zhu, C.C.; Qikun, W.; Xin, L. Large area screen-printing cathode of CNT for FED. *Diam. Relat. Mater.* **2003**, *12*, 1449–1452. [CrossRef]
216. Wang, L.L.; Tay, B.K.; See, K.Y.; Sun, Z.; Tan, L.K.; Lua, D. Electromagnetic interference shielding effectiveness of carbon-based materials prepared by screen printing. *Carbon* **2009**, *47*, 1905–1910. [CrossRef]

217. Sánchez, M.; Rincón, M.E. Sensor response of sol-gel multiwalled carbon nanotubes-TiO_2 composites deposited by screen-printing and dip-coating techniques. *Sens. Actuators B Chem.* **2009**, *140*, 17–23. [CrossRef]
218. Khan, S.; Lorenzelli, L.; Dahiya, R.S. Bendable piezoresistive sensors by screen printing MWCNT/PDMS composites on flexible substrates. In Proceedings of the 2014 10th Conference on Ph.D. Research in Microelectronics and Electronics (PRIME) 2014, Grenoble, France, 30 June–3 July 2014.
219. Tortorich, R.; Choi, J.-W. Inkjet Printing of Carbon Nanotubes. *Nanomaterials* **2013**, *3*, 453–468. [CrossRef]
220. Denneulin, A.; Bras, J.; Carcone, F.; Neuman, C.; Blayo, A. Impact of ink formulation on carbon nanotube network organization within inkjet printed conductive films. *Carbon* **2011**, *49*, 2603–2614. [CrossRef]
221. Song, J.W.; Kim, J.; Yoon, Y.H.; Choi, B.S.; Kim, J.H.; Han, C.S. Inkjet printing of single-walled carbon nanotubes and electrical characterization of the line pattern. *Nanotechnology* **2008**, *19*, 095702. [CrossRef] [PubMed]
222. Beecher, P.; Servati, P.; Rozhin, A.; Colli, A.; Scardaci, V.; Pisana, S.; Hasan, T.; Flewitt, A.J.; Robertson, J.; Hsieh, G.W.; et al. Ink-jet printing of carbon nanotube thin film transistors. *J. Appl. Phys.* **2007**, *102*, 043710. [CrossRef]
223. Chen, P.; Chen, H.; Qiu, J.; Zhou, C. Inkjet Printing of Single-Walled Carbon Nanotube/RuO_2 Nanowire Supercapacitors on Cloth Fabrics and Flexible Substrates. *Nano Res.* **2010**, *3*, 594–603. [CrossRef]
224. Parra-Cabrera, C.; Achille, C.; Kuhn, S.; Ameloot, R. 3D printing in chemical engineering and catalytic technology: Structured catalysts, mixers and reactors. *Chem. Soc. Rev.* **2018**, *47*, 209–230. [CrossRef]
225. Ushiba, S.; Shoji, S.; Masui, K.; Kuray, P.; Kono, J.; Kawata, S. 3D microfabrication of single-wall carbon nanotube/polymer composites by two-photon polymerization lithography. *Carbon* **2013**, *59*, 283–288. [CrossRef]
226. Ghoshal, S. Polymer/Carbon Nanotubes (CNT) Nanocomposites Processing Using Additive Manufacturing (Three-Dimensional Printing) Technique: An Overview. *Fibers* **2017**, *5*, 40. [CrossRef]
227. Acquah, S.F.A.; Leonhardt, B.E.; Nowotarski, M.S.; Magi, J.M.; Chambliss, K.A.; Venzel, T.E.S.; Delekar, S.D.; Al-Hariri, L.A. Carbon Nanotubes and Graphene as Additives in 3D Printing. In *Carbon Nanotubes-Current Progress of Their Polymer Composites*; InTech: Amherst, MA, USA, 2016.
228. Lee, S.J.; Zhu, W.; Nowicki, M.; Lee, G.; Heo, D.N.; Kim, J.; Zuo, Y.Y.; Zhang, L.G. 3D printing nano conductive multi-walled carbon nanotube scaffolds for nerve regeneration. *J. Neural Eng.* **2018**, *15*, 016018. [CrossRef]
229. Cui, H.; Yu, Y.; Li, X.; Sun, Z.; Ruan, J.; Wu, Z.; Qian, J.; Yin, J. Direct 3D printing of a tough hydrogel incorporated with carbon nanotubes for bone regeneration. *J. Mater. Chem. B.* **2019**, *7*, 7207–7217. [CrossRef] [PubMed]
230. Postiglione, G.; Natale, G.; Griffini, G.; Levi, M.; Turri, S. Conductive 3D microstructures by direct 3D printing of polymer/carbon nanotube nanocomposites via liquid deposition modeling. *Compos. Part A Appl. Sci. Manuf.* **2015**, *76*, 110–114. [CrossRef]
231. Ahmed, K.; Kawakami, M.; Khosla, A.; Furukawa, H. Soft, conductive nanocomposites based on ionic liquids/carbon nanotubes for 3D printing of flexible electronic devices. *Polym. J.* **2019**, *51*, 511–521. [CrossRef]
232. Kim, J.H.; Lee, S.; Wajahat, M.; Jeong, H.; Chang, W.S.; Jeong, H.J.; Yang, J.R.; Kim, J.T.; Seol, S.K. Three-Dimensional Printing of Highly Conductive Carbon Nanotube Microarchitectures with Fluid Ink. *ACS Nano* **2016**, *10*, 8879–8887. [CrossRef] [PubMed]
233. Ding, Q.; Liu, M.; Miao, Y.E.; Huang, Y.; Liu, T. Electrospun nickel-decorated carbon nanofiber membranes as efficient electrocatalysts for hydrogen evolution reaction. *Electrochim. Acta* **2015**, *159*, 1–7. [CrossRef]
234. Liu, Y.; Zheng, Y.; Du, B.; Nasaruddin, R.R.; Chen, T.; Xie, J. Golden Carbon Nanotube Membrane for Continuous Flow Catalysis. *Ind. Eng. Chem. Res.* **2017**, *56*, 2999–3007. [CrossRef]
235. Daram, P.; Banjongprasert, C.; Thongsuwan, W.; Jiansirisomboon, S. Microstructure and photocatalytic activities of thermal sprayed titanium dioxide/carbon nanotubes composite coatings. *Surf. Coat. Technol.* **2016**, *306*, 290–294. [CrossRef]